

#### Contents lists available at ScienceDirect

#### Fuel

journal homepage: www.elsevier.com/locate/fuel



#### Full Length Article



## Alternate routes to sustainable energy recovery from fossil fuels reservoirs. Part 1. Investigation of high-temperature reactions between sulfur oxy anions and crude oil

Xiao Jin<sup>a,b</sup>, Jia Wu<sup>a,\*</sup>, Renzo C. Silva<sup>b</sup>, Haiping Huang<sup>b</sup>, Zhihuan Zhang<sup>a</sup>, Ningning Zhong<sup>a</sup>, Benjamin M. Tutolo<sup>b</sup>, Steve Larter<sup>a,b</sup>

#### ARTICLE INFO

# Keywords: Zero carbon emission In-situ fossil fuel recovery Thermochemical sulfate reduction Polysulfide species Mass spectrometry

#### ABSTRACT

The world is undergoing a substantial transition in its energy supply. Examining the possibilities to recover and use fossil fuel energy without emitting carbon dioxide to the surface,  $H_2S$  was considered as an alternative energy vector to deliver a carbon free fuel from petroleum reservoirs to the surface. In this study, we investigated the high P-T chemical oxidation of crude oil with a suite of inorganic sulfur compounds. Tested inorganic sulfur compounds can be ordered by their ability to promote chemical changes to the oil matrix with the concomitant production of hydrogen sulfide, with a reactivity series, listed in order of decreasing reactivity as:  $S^0 > S_2O_3^2 \sim S_4O_6^2 > SO_3^2 > SO_4^2$ . The reaction mechanisms proposed in the study also light on likely key intermediate reactants and the geological timescale process of thermochemical sulfate reduction. Polysulfide species (containing S-S bond structures), such as thiosulfate and tetrathionate, may be reactive intermediates during the redox reaction. However, the early stage of thermochemical sulfate reduction may also involve labile organic sulfur functional groups converting to more stable molecules with aromatic structural units, such as dibenzo-thiophenes (DBT) and benzonaphthothiophenes (BNT). The apparent formation of saturated fatty acids and  $O_2$ , NO and  $O_2$  aromatic heteroatom species indicates the oxidation of saturated and aromatic hydrocarbons or heteroatom compounds. The oxidation of aromatic species may lead to aromatic ring-opening, followed by decarboxylation forming  $O_2$  as final products.

#### 1. Introduction

The world is undergoing a substantial transition in its energy supply and usage, with renewable energy and low carbon energy systems becoming more prevalent. Fossil fuels, however, remain the dominant and major component of the energy supply system. However, if limiting future global warming requires holding atmospheric CO<sub>2</sub> concentrations below a target value, this inexorably leads to the conclusion that most of the world's fossil fuels would have to remain underground, challenging existing economic hierarchies and political systems. One route to addressing this issue has been to examine approaches aimed at recovering the chemical energy stored in reservoir petroleum fluids at the surface, while leaving the carbon in the hydrocarbons in the subsurface [1], enabling petroleum reservoirs to function as decarbonized energy sources. Several potential technologies have been proposed, including in

situ biological or thermal hydrogen generation, direct electricity production in situ, or electricity production at the surface via circulating redox shuttles such as transition metal ions or sulfate-sulfide ion systems [1–3]. A redox shuttle related route involves the oxidation of petroleum fluids in the subsurface by a metal oxide or other species, which in turn is reduced and can be returned to the surface for use in a fuel cell or for direct power generation [4]. Through microbial routes, the sulfate-sulfide system was suggested oxidizing hydrocarbons to form hydrogen sulfide as energy vector.

The process for the sulfate oxidation of organic matter can be considered as: hydrocarbons + SO $_4^{2-} \rightarrow$  CO $_2 +$  H $_2$ S and other reduced S forms + altered hydrocarbons + solid bitumen (or pyrobitumen). Microbial sulfate reduction (MSR, sometimes termed BSR - bacterial sulfate reduction), typically happens at temperatures well below 100 °C and in sulfate-methane transition (SMT) zones within anoxic marine sediments

<sup>&</sup>lt;sup>a</sup> State Key Laboratory of Petroleum Resources and Prospecting, China University of Petroleum (Beijing), Beijing 102249, PR China

b Department of Geoscience, University of Calgary, T2N 1N4, Canada

<sup>\*</sup> Corresponding author at: State Key Laboratory of Petroleum Resources and Prospecting, China University of Petroleum (Beijing), Beijing 102249, PR China. E-mail address: jia.wu@cup.edu.cn (J. Wu).

[5–7]. However, biologically driven routes to sulfate reduction are limited by the toxic nature of sulfide which makes a biological sulfide production route infeasible and difficult to scale in an engineered process [1]. In this paper, as an alternative, we look at the initial stages of assessing the feasibility of using hydrogen sulfide, produced in reservoir by abiotic processes, as a potential carbon free energy vector solution.

Thermochemical sulfate reduction (TSR) to sulfide, coupled with the oxidation of hydrocarbons, is one of the most important organic-inorganic interactions in deep sedimentary basins and is well documented in many geologic environments and experimental studies [8-14]. As TSR is detrimental to oil quality, and ultimately to fluid recovery, because of the high concentrations of H2S and CO2 formed as byproducts, research is generally focused on its mechanism to predict and measure the extent of the TSR-driven crude oil alteration [15-17]. Several studies have used gas chromatography and mass spectrometry techniques (GC-MS) to analyze the extent of alterations in the chemical matrix caused by TSR reactions [18,19]. In particular, Fourier transform ion cyclotron resonance-mass spectrometry (FTICR-MS) has enabled a comprehensive characterization of aromatic and heteroatomic organic compounds present in TSR-altered oils [20,21]. Typically, in the subsurface, petroleum fluids can be oxidized by sulfate ions at temperatures above 110 °C [8], generating CO<sub>2</sub>, H<sub>2</sub>S (and other reduces sulfur species), altered hydrocarbons and solid bitumen. There are three main mechanistic steps hypothesized in TSR reactions [17]. Initially, at a slow rate, sulfate reduction by hydrocarbons forms more reactive intermediate inorganic sulfur species such as sulfite and polysulfide species, whereas in the petroleum matrix, oxidized intermediates such as hydroxylated compounds are formed [22]. Then, these intermediate species undergo further transformation, eventually completely reducing sulfur oxy anions and yielding H2S, CO2, altered hydrocarbons and solid bitumen. Finally, the generated H2S acts as a catalyst and back reacts with hydrocarbons to form additional labile organosulfur compounds (OSC), which are allegedly more reactive and further promote TSR in the petroleum fluid. Given the constant production of H2S, TSR reactions in such conditions are said to be auto-catalyzed [17].

However, TSR is not efficient in natural settings and only occurs in relatively hot petroleum reservoirs with threshold temperatures as high as 140 °C being claimed [11], over long geological timescales [23]. A relatively high activation energy barrier for such reactions relates to the required cleavage of the first S-O bond in sulfate leading to the formation of sulfite [16,23,24]. For an engineered solution where rapid thermochemical oil oxidation is targeted, externally added inorganic sulfur species other than sulfate might be used to accelerate the overall process. In this paper, the first of a series, we look at experiments designed to better understand the mechanistic aspects of the S<sub>x</sub>O<sub>v</sub>-hydrocarbon reaction system to see if there are routes to accelerate an inreservoir hydrocarbon oxidation process using sulfur species. This would potentially enable the use of sulfur species-crude oil reactions to produce hydrogen sulfide from petroleum reservoirs at scale as an energy vector, on human timescales. While hydrogen sulfide is toxic and corrosive, the petroleum industry has safely dealt with sour streams of hydrocarbon fluids for decades, with most of the extracted processed sulfur considered a residual by-product.

In the study reported here, high-temperature, high-pressure experiments, under hydrous pyrolysis conditions, were conducted using mixtures of crude oil, water and five different sulfur-containing inorganic species ( $SO_4^{2-}$ ,  $SO_3^{2-}$ ,  $S_2O_3^{2-}$ ,  $S_4O_6^{2-}$ ,  $S_8$ ), to investigate the efficiency of such organic–inorganic interactions, monitored by the generated gases and the alterations in the petroleum chemical matrix as measured via GC–MS and FTICR-MS. Mechanistic insights and other factors that could enhance oil oxidation in TSR-like reactions are presented and discussed in the context of both a technological process and geological timescale TSR.

#### 2. Methods

#### 2.1. Experimental design

One crude oil sample from the Shengli Oilfield (API gravity  $=40^{\circ}, S=0.68$  %wt.), Eastern China, was used as the base oil for this study. Oil samples were subjected to hydrous pyrolysis experiments at 360 °C in the presence of different sulfur compounds: sulfate (SO $_4^2$ ), sulfite (SO $_3^2$ ), tetrathionate (S $_4$ O $_6^2$ ), thiosulfate (S $_2$ O $_3^2$ ), and elemental sulfur. MgSO $_4$  (Innochem, >98%), Na $_2$ S $_4$ O $_6$ :2H $_2$ O (Innochem, >98%), Na $_2$ S $_0$ 3 (Adamas-beta, >98%), Na $_2$ S $_0$ 3:5H $_2$ O (FengChuan, >99%) and S $_8$  (Alfa Aesar, >99.5%). Table 1 shows the inorganic sulfur compounds used in these experiments and their oxidation states. Control experiments without a sulfur source were also conducted. Table 2 lists sample codes and experimental conditions for the 22 experiments reported in this study.

#### 2.2. High-temperature high-pressure experiments

All high-temperature high-pressure experiments were conducted at the State Key Laboratory of Petroleum Resources and Prospecting, using gold tubes as the reaction chamber, subjected to conditions common in hydrous pyrolysis experiments [see Fig. S1; 25]. Each gold tube (60 mm length, 5 mm o.d., 0.25 mm thick) was sealed on one end by argon arc welding. After loading the contents (Table 2), the tube was flattened to reduce the volume of empty space inside. Then, the open end was also welded using an argon arc, while the tube contents were flushed with argon. The structural integrity of the reaction capsule during the experiments, was examined by verifying whether there was any weight loss after the experiments. In each experiment, the temperature of the cell was programmatically increased from ambient to 360 °C within 1 h, and the confining pressure was kept at 450 bar. The time recording was started as soon as the cell temperature reached the target temperature, and the high-temperature and high-pressure conditions were maintained for 72 h. Samples were then left at room temperature and pressure to cool down for approximately 4 h.

#### 2.3. Gas analysis

At room temperature, gases from the capsules were individually collected inside a calibrated volume auxiliary cylinder, which was equilibrated at below  $10^{-3}$  bar before piercing the gold tube. Once the capsules are pierced, the resultant increase in the inner pressure of the cylinder was recorded. This pressure increase was then used to calculate the total amount of gas products trapped inside the gold tube based on the assumption of ideal gas behavior [26]. Approximately 5 mL of the collected gas was transferred to the gas chromatograph using a plastic syringe. Due to the toxicity of  $H_2S$  leading to the risk to human health, the experiments were completed in a fume hood. A sodium hydroxide solution was used to remove the  $H_2S$  released in the GC exhaustion port.

Each gas compound was identified and quantified on a two-channel Agilent 7890 Series Gas Chromatograph integrated with an auxiliary oven, which was custom-configured by Wasson-ECE Instrumentation. The instrument was equipped with two capillary and six packed

Table 1 Inorganic sulfur compounds formula, and net sulphur oxidation state. Experiments using these compounds were labeled as "Exp.  $ID_X$ ", where X is substituted by the experiment number.

Compound name	Formula	S Oxidation state	Exp. ID
Sulfate	$SO_4^{2-}$	+6	Sulfate_X
Sulfite	$SO_3^{2-}$	+4	Sulfite_X
Tetrathionate	$S_4O_6^{2-}$	+2.5	Tetra_X
Thiosulfate	$S_2O_3^{2-}$	+2 (+6, -2)	Thio_X
Elemental sulfur	$S_8$	0	Sulfur_X

Table 2
Experimental designs used for the high-pressure, high-temperature experiments conducted at 360 °C, 450 bars for 72 h. In all experiments, 300 uL of water was also included in the reaction chamber. Headspace gases were analyzed by GC-TCD and GC-FID. \*Samples analyzed by FTICR-MS.

Exp. ID	Oil (mg)	SO <sub>4</sub> <sup>2-</sup> mmol	$\mathrm{SO}_3^{2-}$	$S_2O_3^{2-}$	$S_4O_6^{2-}$	S	H <sub>2</sub> S mg/g Oil	$CO_2$	CH <sub>4</sub>	$C_2H_6$	C <sub>3</sub> H <sub>8</sub>	$C_1 \sim C_5$
Sulfate_1*	113.5	1.01	-	-	-	-	9.10	0.00	6.62	4.02	5.77	24.94
Sulfate_2	184.1	0.97	_	_	_	_	6.61	0.04	1.90	3.43	6.52	22.01
Sulfite_1*	154.1	_	1.37	_	_	_	5.69	0.04	12.03	9.21	12.64	51.27
Sulfite_2	128.7	_	1.02	_	_	_	8.59	0.07	3.05	2.88	5.18	24.99
Thio_1*	211.6	_	_	0.65	_	_	97.12	19.75	21.19	17.14	18.86	71.37
Thio_2	199.2	_	_	0.59	-	_	89.62	11.46	9.36	6.04	6.34	26.17
Thio_3	207.0	_	_	0.58	-	_	38.29	5.81	7.11	4.35	4.74	19.99
Thio_4	132.2	_	_	0.27	-	_	56.48	7.46	6.36	3.77	4.18	18.12
Thio_5	282.7	_	_	0.29	_	_	12.49	2.08	4.45	1.69	1.57	8.97
Thio_6	125.4	_	_	0.16	_	_	32.50	4.63	5.78	2.94	3.04	14.41
Tetra_1*	191.2	_	_	_	0.41	_	79.14	31.90	23.03	19.32	19.50	75.24
Tetra_2	103.1	_	_	_	0.45	_	177.95	36.50	14.49	17.09	22.52	76.99
Tetra_3	223	_	_	_	0.82	_	74.44	10.97	4.59	1.88	1.93	9.65
Tetra_4	239.6	_	_	_	0.64	_	36.37	11.86	3.85	1.10	0.79	6.18
Tetra_5	186.7	_	_	_	0.35	_	51.54	9.46	6.51	4.26	4.13	17.83
Tetra_6	216.4	_	_	_	0.32	_	34.70	6.74	5.51	3.06	2.77	13.30
Tetra_7	119.7	_	_	_	0.22	_	51.04	10.97	7.70	4.95	4.23	19.84
Tetra_8	167.9	_	_	_	0.21	_	26.95	4.82	3.66	1.51	1.30	7.45
Sulfur_1*	244.1	_	_	_	-	2.39	155.62	30.15	10.25	8.09	10.68	39.32
Sulfur_2	136.0	-	_	-	-	3.17	580.33	61.23	5.18	4.58	5.27	19.43
Oil_360_1*	186.2	-	_	-	-	-	1.26	1.90	3.15	1.08	0.94	5.93
Oil_360_2	113.7	-	_	-	-	-	0.00	2.05	2.73	1.70	2.52	11.27
Oil_Ini*	_	_	-	-	_	-	_	-	-	-	-	_

analytical columns, a flame ionization detector (FID) and two thermal conductivity detectors (TCD). The carrier gases for FID and TCD were high-purity  $N_2$  and He, respectively. The temperature of the GC oven was programed as follows: 68 °C for 7 min, from 68 °C to 90 °C at a linear rate of 10 °C/min, 90 °C for 1.5 min, from 90 °C to 175 °C at a linear rate of 15 °C/min, and finally 175 °C for 5 min. Calibration of chromatograph response was performed with external gas standards, each of which was prepared at a precision of less than  $\pm$  1 mol% [27]. The scheme of gas analysis was shown in Fig. S2.

#### 2.4. GC-MS analysis

Following the completion of gas analysis, the gold tube was transferred to a clean vial filled with dichloromethane, and then sliced into 2–5 pieces. Vials were capped and sonicated 3  $\times$  5 min. Contents were filtered to remove and recycle the gold residuals, and the oil filtrate was collected and air-dried.

Samples spiked with a suite of internal standards (d<sub>8</sub>-naphthalene,  $d_{10}$ -phenanthrene, 1,1'-binaphthyl, squalene,  $d_{16}$ -adamantane,  $d_{4}$ -cholestane) were separated into fractions using a small-scale column (pipette) liquid chromatography method [28]. The saturated and aromatic hydrocarbon fractions were analyzed without solvent evaporation by gas chromatography-mass spectrometry (GC-MS). The GC-MS analysis of molecular markers was carried out on an Agilent 5977A Mass Spectrometer, coupled with an Agilent 7890B Gas chromatography equipped with a HP-5MS fused silica capillary column (30 m  $\times$  0.25 mm i.d.) with a 0.25-µm coating. Helium was used as the carrier gas. The oven temperature was initially set at 40 °C for 5 min, programmed to 325 °C at 4 °C/min and held for 15 min. The ion source was operated in the electron impact ionization (EI) mode at 70 eV, and the detector was operated in both scan (m/z 50 – 500) and single-ion monitoring mode (m/z 85 - 365). Quantification of compounds were conducted using peak areas relative to the most appropriate internal standard, squalene for acyclic alkanes, d4-cholestane for naphthenic alkanes and d8-naphthalene,  $d_{10}$ -phenanthrene, 1,1'-binaphthyl for aromatic hydrocarbons. No response factor calibration for individual compounds has been applied in this study, response factors for all species being assumed to be one.

#### 2.5. FTICR-MS analysis

A subset of 6 pyrolysate samples (identified in Table 2) and the original oil were selected for FTICR-MS analysis, using two ionization modes: atmospheric pressure photoionization operating in positive ion mode, (+) APPI, and electrospray ionization operating in negative ion mode, (-) ESI.

For the analysis using (+) APPI, whole oils were diluted to 0.25 mg/ mL in toluene and then infused into the ionization source using a syringe pump set to deliver 200  $\mu$ L/h. A krypton lamp at 10.6 eV was used as the ion source. Transfer capillary temperature and nebulizer pressure were set to 350 °C and 1.0 bar, respectively. For analysis (-) ESI, whole oils were diluted to 0.25 mg/mL in methanol:toluene (1:1) and then infused into the ionization source using a syringe pump set to deliver 200  $\mu$ L/h. Transfer capillary temperature and nebulizer pressure were set to 200 °C and 0.5 bar, respectively. Reserpine (C33H40N2O9) was added to the sample solutions to assist with mass spectra calibration. Ions ranging from m/z 150 to 1500 were isolated with a linear quadrupole and accumulated over 1-10 ms in the collision cell, before being transferred to the ion cyclotron resonance cell. Two hundred transients of 8 million points in the time domain were collected in absorption mode and summed to improve the experimental signal/noise ratio (SNR). In this configuration, the SolariX mass resolving power is higher than 2,000,000 at m/z 400. Samples were analyzed in a randomized order to minimize the impact of any potential instrumental drift during the

Raw FTICR-MS data were processed using CaPA v.1.0 (Aphorist Inc.) software. Peaks with SNR higher than 5 were assigned to a molecular formula based on highly accurate m/z measurements and on stable isotope occurrence, whenever possible. Compositional boundaries, in terms of stoichiometry for the species fitting algorithm, were set to C<sub>4</sub>.  $_{80}$ H<sub>4-200</sub>N<sub>0-2</sub>S<sub>0-2</sub>O<sub>0-4</sub> and C<sub>4-80</sub>H<sub>4-200</sub>N<sub>0-2</sub>S<sub>0-2</sub>O<sub>0-5</sub>Na<sub>0-1</sub>Cl<sub>0-1</sub> for (+) APPI and (-) ESI analyses, respectively. Double bond equivalent (DBE) range, which is a measure of molecular hydrogen deficiency due to double bonds and/or cyclic structures, was set between -1 and 50. Each mass spectrum was recalibrated using homologous series present in the sample. Any peak detected in the solvent blanks with relative intensity higher than 1% of the base peak had their intensities set to zero in sample spectra. Compound classes with<10 and 40 detected peaks in (+) APPI and (-) ESI, respectively, are not discussed. Molecular formulae

were assigned with absolute errors lower than 600 ppb.

The resulting list of molecular formulae and intensities is typically analyzed by summarizing the data based on three non-hierarchical layers: heteroatom class, DBE and carbon number. Heteroatom class describes the amount of the heteroatoms contained in a given molecular formula. The symbol "HC" is used for the class in which when no heteroatom is present in the molecular formula. In this study, unless otherwise mentioned, in (+) APPI mode, the intensities of a given molecular formula detected as radical and protonated ion are combined.

#### 2.6. Sulfur oxy anions geochemical modelling

Geochemist's Workbench [29] outfitted with a custom thermodynamic database produced using the DBCreate software package was used to calculate expected concentrations of sulfur oxy anions species and other intermediates under reaction at 360 °C and 450 bars [30]. Thermodynamic data for sulfur species were taken from Shock et al. 1997 and thermodynamic properties of hydrocarbon species were taken from Shock et al. 1990 [31,32]. 1-Octene ( $C_8H_{16}$ ) was used to as a model species to simulate the interaction between hydrocarbons and sulfate. The initial molality of sulfur oxy anions ( $SO_4^2$ ,  $SO_3^2$ .  $S_2O_3^2$ ,  $S_4O_6^2$  and  $S_8^0$ ) and  $C_8H_{16}$  in these model experiments were 1.47 mol/kg in water.

#### 3. Results

#### 3.1. Yields of H<sub>2</sub>S, CO<sub>2</sub> and CH<sub>4</sub>

The sealed reaction tubes showed no mass losses after the high temperature-high pressure experiments. Minute amounts of H<sub>2</sub> could be detected when treating oil with sulfate, sulfite or when no sulfur compounds were added. Gas analysis results for C<sub>1-5</sub> hydrocarbons, H<sub>2</sub>S and CO<sub>2</sub> are shown in Table 2. Most analyses showed hydrogen yields below the limit of detection, except for samples containing sulfate and sulfite (at 0.46 and 0.06 mg/g oil, respectively). Hydrogen in the reaction chamber is likely to be an intermediate produced from the dehydrogenation of hydrocarbons, or from reforming reactions and would likely be readily consumed to form more saturated species or H2S. Yields of H2S, CO2 and CH4 normalized to the amount of sulfur added to the reaction chamber are shown in Fig. 1. Negligible amounts of H2S and CO2 are detected when no S-containing reactant is added (Oil\_360 samples), and yields of these compounds are also low in reactions with sulfate and sulfite (Fig. 1a). H<sub>2</sub>S formation could be detected in all experiments but to a lower extent in Oil 360 (experiments with oil carried out at 360 °C) experiments. A positive correlation exists between the H<sub>2</sub>S yield and the concentration of sulfur added to the system (Fig. 1a;  $R^2_{thiosulfate} = 0.96$ ,  $R^2_{tetrathionate} = 0.68$ ). In experiments with sulfate, sulfite and also in Oil 360 experiments, CO<sub>2</sub> was only detected at yields lower than 2 mg/g oil (Table 2, Fig. 1b). CO2 yield also correlates with the absolute concentration of sulfur added to the system (Fig. 1b). The highest H<sub>2</sub>S and CO<sub>2</sub> yields are observed in the experiments using elemental sulfur. The uncertainty analysis of the yields of H2S and CO2 was conducted on experiments with similar ratios of mole of S/mass of oil, which shown in Table 3 and Fig. 2. The standard deviation of the yield of both H<sub>2</sub>S and CO<sub>2</sub> were<0.004. The relative errors of the yield of H<sub>2</sub>S are 0.9%–8%; the yields of  $CO_2$  are 7%–26%. There is no linear correlation ( $R^2 = 0.02$ ) between the yield of CH<sub>4</sub> and the concentration of sulfur (Fig. 1c). The highest CH4 yields (and gaseous hydrocarbons yields in general), are detected in experiments with tetrathionate and thiosulfate.

#### 3.2. Molecular markers analysis by GC-MS

The  $C_{11.38}$  n-alkane distributions of the original and altered oils, as measured by GC–MS, are shown in Fig. 3. All the altered oils, except the one altered with sulfate, exhibit an n-alkane distribution shifted towards lower homologs after hydrous pyrolysis, compared to the initial oil and altered oil without sulfur oxy anions. The original oil shows the lowest

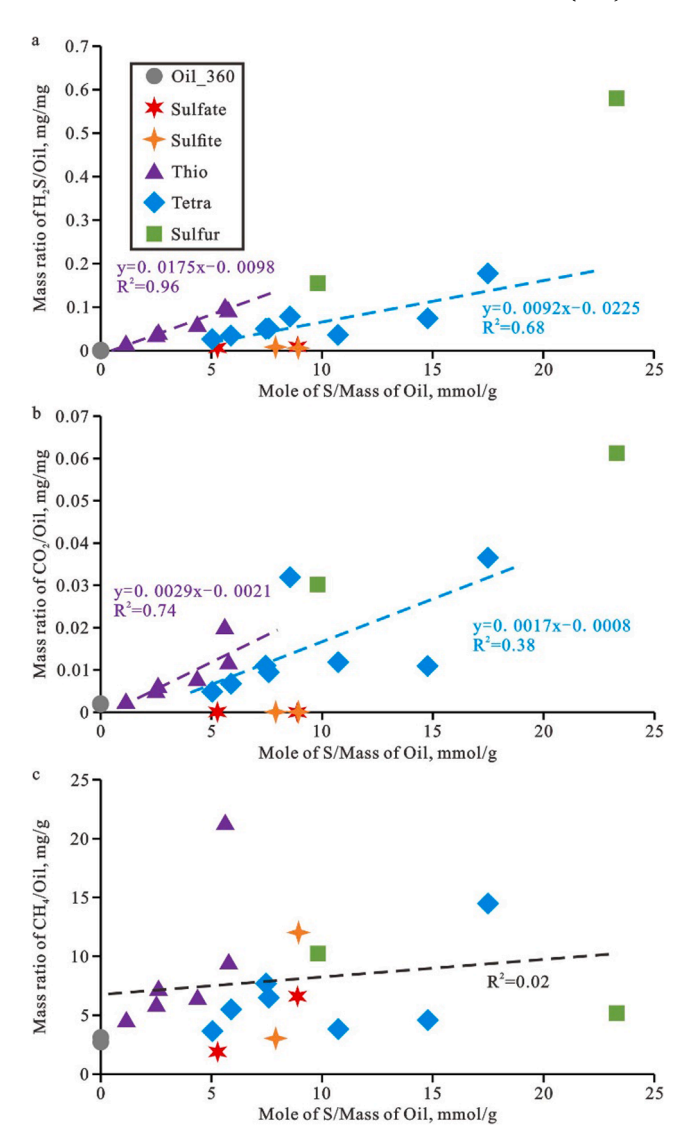


Fig. 1. Formation yields of (a)  $H_2S$ , (b)  $CO_2$ , and (c)  $CH_4$ , as a function of the amount of inorganic sulfur added in the reaction chamber. Data points are color- and shape-coded based on the added sulfur compound (refer to Table 2 for full experimental details). "Oil" represents samples with no sulfur added: Oil\_360\_1 and Oil\_360\_2 from Table 2). Each experimental point represents one measurement.

 $n{\rm C}_{21-}/n{\rm C}_{22+}$  ratio of the set (0.84) while altered samples showed  $n{\rm C}_{21-}/n{\rm C}_{22+}$  ratios between 0.92 and 1.65 (Table 4). In all experiments, the concentrations of pristane and phytane decrease relatively to  $n{\rm C}_{17}$  and  $n{\rm C}_{18}$ , respectively, compared to the initial oil and the control Oil\_360 experiment, suggesting relatively higher rates of reactivity for branched chain versus linear hydrocarbons.

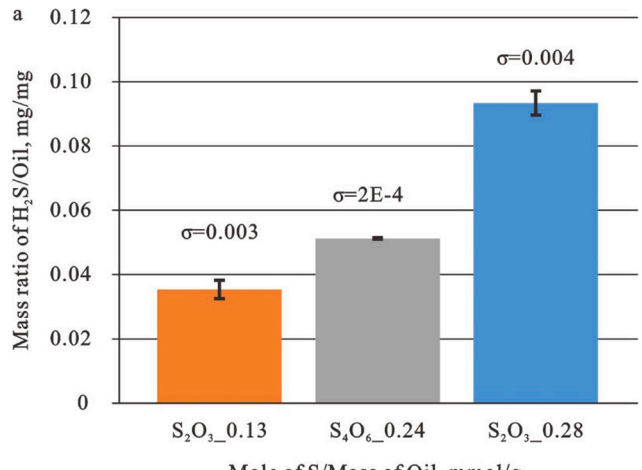
Biomarker alkane compounds such as  $C_{30}$ -hopane and  $C_{27}$ - $\alpha\alpha\alpha R$ -sterane also showed reduced concentrations after pyrolysis, in experiments with added sulfur compounds. For example, the concentration of  $C_{30}$ -hopane varied from 2223.83 ppm to 1190.00 ppm and then to 0.89 ppm: initial oil, heated oil without S species and altered oil with  $S_8$  (Experiments: Oil\_Ini, Oil\_360\_1 and S\_1 in Table 4). Other biomarkers like the  $C_{29}$ - $\alpha\alpha\alpha R$ -sterane are below the limit of detection in oils reacted with added sulfur compounds.

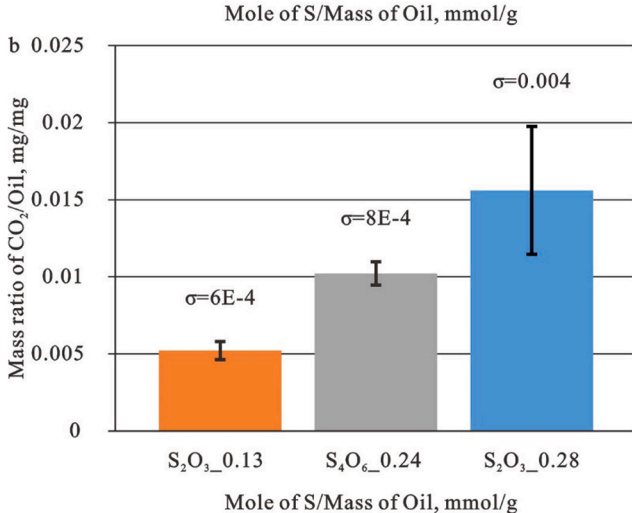
Elemental sulfur (Fig. 4a) was detected in both saturated hydrocarbon and aromatic hydrocarbon fractions in all altered oils except for the Oil\_360 experiment. Results for labile organosulfur compounds, detected in the aromatic fraction of altered oils, such as  $S_5C_2H_4$  (pentathiepane, TIC, Fig. 4b) and  $S_6CH_2$  (hexathiepane, m/z 142, Fig. 4c), are also

Table 3 Uncertainty analysis of the yields of  $H_2S$  and  $CO_2$  from the oxidation of oil by  $S_2O_3^{2-}$  and  $S_4O_6^{2-}$ .

Inorganic S species	Oil mg	S species mg	Mole of S/mass of oil	H <sub>2</sub> S mg/g oil	Relative Error	$CO_2$ mg/g oil	Relative error
$S_2O_3^{2-}$	211.6	147.4	0.28	97.12	4%	19.75	26%
$S_2O_3^{2-}$	199.2	142.7	0.29	89.62	4%	11.46	26%
$S_2O_3^{2-}$	207.0	66.9	0.13	38.29	0.9%	5.81	7%
$S_2O_3^{2-}$	125.4	39.1	0.13	32.50	0.9%	4.63	7%
$S_4O_6^{2-}$	186.7	108.5	0.24	51.54	8%	9.46	11%
$S_4O_6^{2-}$	119.7	68.3	0.24	51.04	8%	10.97	11%

 $\text{Relative errors} = \frac{\left| \textit{YieldofGas} - \textit{Yieldofgas}_{\textit{ave}} \right|}{\textit{Yieldofgas}_{\textit{ave}}}$ 





**Fig. 2.** Uncertainty analysis of the yields of  $H_2S$  and  $CO_2$  from the oxidation of oil by  $S_2O_3^{2-}$  and  $S_4O_6^{2-}$ .  $\sigma=$  standard deviation; the error bar indicates the relative error.

reported in Table 4. Experiments with sulfite showed a remarkably high concentration of pentathiepane. Dibenzothiophene (DBT) and benzonaphthothiophene (BNT) were quantified in the aromatic fraction of all samples (Table 4), and the lowest concentrations of these compounds were found in the original oil (19.58 and 27.13 ppm, respectively), followed by the Oil\_360 experiment. The concentration of DBT and BNT in altered oils increases by 5 to 20 times in experiments with added sulfur compounds.

#### 3.3. Heterocompound analysis by FTICR-MS

Heteroatom containing species were monitored using FTCIR-MS. In all mass spectra acquired in this study, only singly charged species were detected as indicated by the isotopic pattern of  $^{13}$ C peaks. In (+) APPI

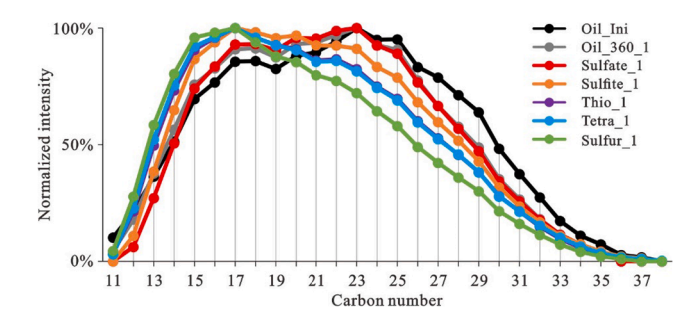


**Fig. 3.** n-Alkane distribution in original and altered oils, as measured by GC–MS (m/z 85). The intensity was normalized to the highest peak in the series for each sample. In this figure, only the oils selected for FTICR-MS analyses are shown (see Table 2).

mode, typically<3% of the total peak intensity in a spectrum was left unassigned, whereas in (-) ESI mode, due to the presence of background contaminants, up to 25% of the total peak intensity could be left unassigned. Solvent blank analysis identified 115 and 220 peaks respectively with relative intensity higher than 1% in (+) APPI and (-) ESI mode analysis, and these peaks had their intensities set to 0 whenever identified in the sample runs. The vast majority of monoisotopic peaks were assigned to molecular formulae with molecular mass errors lower than 200 ppb in both ionization modes (see Fig. S3). Despite providing unambiguous molecular formula for detected peaks, structural discussions on individual species can only be speculative as FTICR-MS data ultimately does not distinguish isomers, so only gross structural style inferences are possible. Also, quantitative aspects are not considered in this study, thus intensities reported herein are not assumed to reflect the actual concentration of compounds in the sample, but the comparison of relative intensities between different species is useful and can reflect general related changes occurring in detected species within the sample matrix.

Fig. 5 shows the overall heteroatom class, DBE and carbon number distribution assessed in the samples using (+) APPI FTICR-MS. Species detected as radical and protonated ions are not differentiated here, thus their intensities are combined within their heteroatom class. The major heteroatom classes detected are hydrocarbons (HC), as well as species containing S<sub>1</sub>, N<sub>1</sub>, and O<sub>1</sub>, accounting for>90% of sample total intensities (Fig. 5a and Table S1). The initial oil sample and oil pyrolyzed at 360 °C (Oil\_Ini and Oil\_360) show the highest abundance of class HC, and the lowest class O relative intensities. Detected species in (+) APPI mode ranged from  $C_{10-75}$  (m/z 150 to 1050) and DBE 1-36. All reacted samples show a smoother carbon number distribution profile compared to the more discontinuous profile with C<sub>27-30</sub> and C<sub>40</sub> relatively elevated peak intensity shown by the initial oil sample (Oil-Ini; Fig. 5b). Samples altered by reaction with  $S_2O_3^{2-}$ ,  $S_4O_6^{2-}$  and  $S^0$  are the ones most distinct from Oil\_360 (control sample with no sulfur species present), with elevated relative intensities of components towards lower carbon numbers. Similarly, Oil\_360 is distinguished from other altered oils by exhibiting compounds with generally lower DBE values (Fig. 5c). The major heteroatom classes detected in (+) APPI also have their classExperimental designs used for the high-pressure high-temperature experiments conducted at 360 °C, 450 bars for 72 h. In all experiments, 300 µL of water was included in the reaction chamber. All resulting altered oils were analyzed by GC-MS and some molecular abundance ratios and absolute compound concentrations are also shown. \*Samples analyzed by FTICR-MS. DBT = dibenzothiophene, DBF = dibenzofuran, BNT = ben-

X. Jin et al. Fuel 302 (2021) 121050

Exp. ID	Oil	$50_{4}^{2-}$	$\mathrm{SO}_3^{2-}$	$\mathrm{S_2O_3^{2-}}$	$S_40_6^{2-}$	S	$nC_{21}$ - $/nC_{22}$ +	Pr/Ph	$Pr/nC_{17}$	$Ph/nC_{18}$	$\mathcal{S}_0$	$S_5C_2$	$S_{6}C$	DBT	DBF	BNT	$C_{30}H$	$C_{27}\alpha\alpha\alpha R$
	mg	mmol									μg/g Oil							
Sulfate_1*	113.5	1.01					0.97	0.43	0.40	0.92	0.90	6.03	0.93	85.91	17.11	101.04	30.49	26.43
Sulfate_2	184.1	0.97	ı	1	ı	1	1.13	0.46	0.27	0.59	5.88	7.80	2.02	96.32	19.20	63.51	4.12	9.30
Sulfite_1*	154.1	ı	1.37	ı	ı	1	1.17	0.50	0.22	0.46	0.01	1948.47	15.35	351.09	93.61	310.94	7.86	12.28
Sulfite_2	128.7	ı	1.02	1	ı	1	1.30	0.53	0.17	0.33	1.17	2361.38	91.78	338.22	109.77	330.53	7.70	9.57
$Thio_1^*$	211.6	ı	ı	0.65	ı	1	1.35	0.48	0.11	0.24	19.74	112.24	89.9	248.07	42.26	244.05	1.31	5.07
Thio_2	199.2	1	ı	0.59	ı	1	1.00	0.43	0.44	1.03	8.98	52.84	6.78	142.78	31.94	140.32	1.79	11.66
Thio_3	207.0	ı	ı	0.58	ı	ı	1.03	0.44	0.45	1.02	3.19	4.74	1.08	99.34	23.68	106.88	4.84	16.88
Thio_4	132.2	ı	ı	0.27	ı	ı	0.99	0.42	0.47	1.10	2.89	54.83	2.59	108.59	24.12	114.20	16.79	21.39
Thio_5	282.7	ı	ı	0.29	ı	1	0.99	0.45	0.52	1.17	0.92	8.05	0.48	52.53	16.08	64.33	78.35	42.93
Thio_6	125.4	ı	ı	0.16	ı	1	0.98	0.44	0.50	1.14	1.42	23.67	1.26	84.37	19.93	84.84	84.11	46.37
Tetra_1*	191.2	ı	ı	1	0.41	1	1.36	0.48	0.11	0.23	86.9	26.48	3.94	195.14	30.49	226.29	1.27	5.27
Tetra_2	103.1	ı	ı	ı	0.45	1	1.09	0.44	0.21	0.48	3.85	10.36	2.04	201.76	26.76	238.19	3.40	5.01
Tetra_3	223	ı	ı	I	0.82	ı	0.95	0.42	0.53	1.27	5.22	22.68	5.79	100.01	20.34	89.14	36.40	29.96
Tetra_4	239.6	ı	ı	ı	0.64	ı	0.94	0.42	0.54	1.29	80.9	3.85	0.72	101.19	23.71	85.04	68.58	44.42
Tetra_5	186.7	ı	ı	I	0.35	ı	1.05	0.44	0.49	1.14	1.22	3.73	1.31	71.87	16.76	88.90	13.17	25.60
Tetra_6	216.4	ı	ı	ı	0.32	ı	0.99	0.43	0.51	1.19	2.36	6.04	2.11	63.82	16.60	78.51	30.87	32.12
Tetra_7	119.7	ı	ı	ı	0.22	ı	0.95	0.42	0.49	1.15	1.08	5.85	1.37	69.71	15.19	83.05	26.94	26.65
Tetra_8	167.9	1	1	ı	0.21	ı	1.03	0.44	0.55	1.27	1.13	4.69	0.88	53.81	16.28	72.20	154.71	06.09
$Sulfur_1^*$	244.1	ı	ı	ı	I	2.39	1.65	0.49	80.0	0.16	6.13	22.13	8.08	464.31	32.35	333.05	0.89	5.47
Sulfur_2	136.0	ı	ı	I	I	3.17	0.92	0.39	0.43	1.09	0.29	17.23	4.18	231.69	17.44	129.58	16.79	6.87
Oil_360_1*	186.2	ı	ı	I	I	ı	0.99	0.42	0.56	1.31	0.05	p.u	n.d	30.24	14.56	47.90	1190.00	184.52
Oil_360_2	113.7	ı	ı	I	I	ı	0.92	0.43	0.53	1.23	0.20	p.u	n.d	28.90	10.67	56.93	1053.61	188.89
Oil Ini*	ı	1	1	ı	ı	ı	0.84	0.40	09.0	1.52	n.d.	p.u	n.d	19.58	11.48	27.13	2223.83	492.63

specific carbon and DBE distribution also shown in Fig. 5d–k. In thio-sulfate, tetrathionate and elemental sulfur reacted oils, barely any species are detected in class  $S_1$  DBE < 6, class  $O_1$  DBE < 9, class  $N_1$  DBE < 9. Note that the FTICR-MS technique as applied herein cannot detect ions < m/z 150.

Fig. 6. shows the same heteroatom species reported in Fig. 5 for the (-) ESI FTICR-MS data. The (-) ESI spectra are dominated by heteroatom class  $N_1$  species, followed by, in no particular order,  $O_1$ ,  $O_2$ , NO, and NS species (Fig. 5a and Table S2). These heteroatom classes have their carbon number and DBE distribution plots shown in Fig. 6b-n. Both overall carbon number and DBE distributions ranges detected in (-) ESI spectra are similar to those reported for (+) APPI data.

#### 3.4. Calculation of sulfur oxy anion reactivity and active speciation

To assess possible inter-species equilibration and reactivity with hydrocarbons for sulfur anions, the Geochemist's Workbench (GWB) was used to carry out some preliminary simulations. The molality (the moles of solute in 1 kg of solvent; mol/kg) of intermediate sulfurcontaining species likely to exist under 360 °C, 450 bars for 72 h were shown in Table 5. When simulating only the sulfate in water under high P-T, most of S-containing species are in the form of sulfate. As for other reactive sulfur-containing species in water, significant abundance of  $SO_2(aq)$  and  $S_2O_3^{2-}$  should exist after heating. When we add 1-Octene to sulfate (both are 1.47 mol/kg) under high P-T, the results suggested most S-containing species would transform to H<sub>2</sub>S(aq) and HS<sup>-</sup>. Polysulfide species, such as  $S_2^{2-}$  and  $S_3^{2-}$  are also suggested to possibly coexist in water. While the results are preliminary and not confirmed by direct analysis, they suggested that thiosulfate and tetrathionate ions may produce polysulfide species in solution under the experimental conditions. Interconversion of sulfur oxy anions to more reactive polysulfide species may be an important factor in reactivity in lab and even field settings.

#### 4. Discussion

#### 4.1. The efficiency of sulfur oxy anions for hydrocarbon oxidation

As in general, the yield of H<sub>2</sub>S correlates positively with the quantity of sulfur added into reaction chamber (Fig. 1a), we observe that the linear slope of H<sub>2</sub>S yield indicates the conversion efficiency of sulfur elements in any form to H<sub>2</sub>S during pyrolysis. Based on the conversion ratio of S atoms to H<sub>2</sub>S, the overall hydrogen sulfide productivity sequence for the experiments involving sulfur bearing compounds is: S<sup>0</sup> > S<sub>2</sub>O<sub>3</sub><sup>2</sup> > S<sub>4</sub>O<sub>6</sub><sup>2</sup> > SO<sub>3</sub><sup>2</sup>  $\approx$  SO<sub>4</sub><sup>2</sup>. It should be noted however, that H<sub>2</sub>S can also be derived from the disproportionation of multiple S anions, as for example [33,34]:

$$8S^{x+} \, + \, 4(x+2)H_2O \stackrel{\Delta}{\to} (x+2)SO_4^{2-} \, + (6-x)H_2S \, + (10x+4)H^+$$

Therefore,  $H_2S$  yield alone should not be used to probe the efficiency of the proposed oil oxidation reactions, unless its source processes can be accurately decoupled, which is not the case using the setup reported herein. The "apparent reactivity series", is however qualitatively useful. The  $CO_2$  yield in the experiments is perhaps a better proxy for the reaction extent. Redox reactions alone may not be directly causing all  $CO_2$  formation as the high-temperature experimental conditions used herein also favor decarboxylation processes or even some direct waterhydrocarbon reactions. Still, any oxygenated species formed during the redox reactions may eventually result in released  $CO_2$  thus making  $CO_2$  yield an indirect proxy of extent of reaction.

A positive relationship has been observed between the  $CO_2$  yield and concentration of added sulfur in the reaction chamber (Fig. 1b). The  $CO_2$  yields can only reach 1/5 of the  $H_2S$  yields as measured by a linear fit in the thiosulfate and tetrathionate experiments (Fig. 7), which further suggest that part, if not the majority, of the added sulfur reacts with water rather than organic species. Based on the yield of  $CO_2$ , the relative

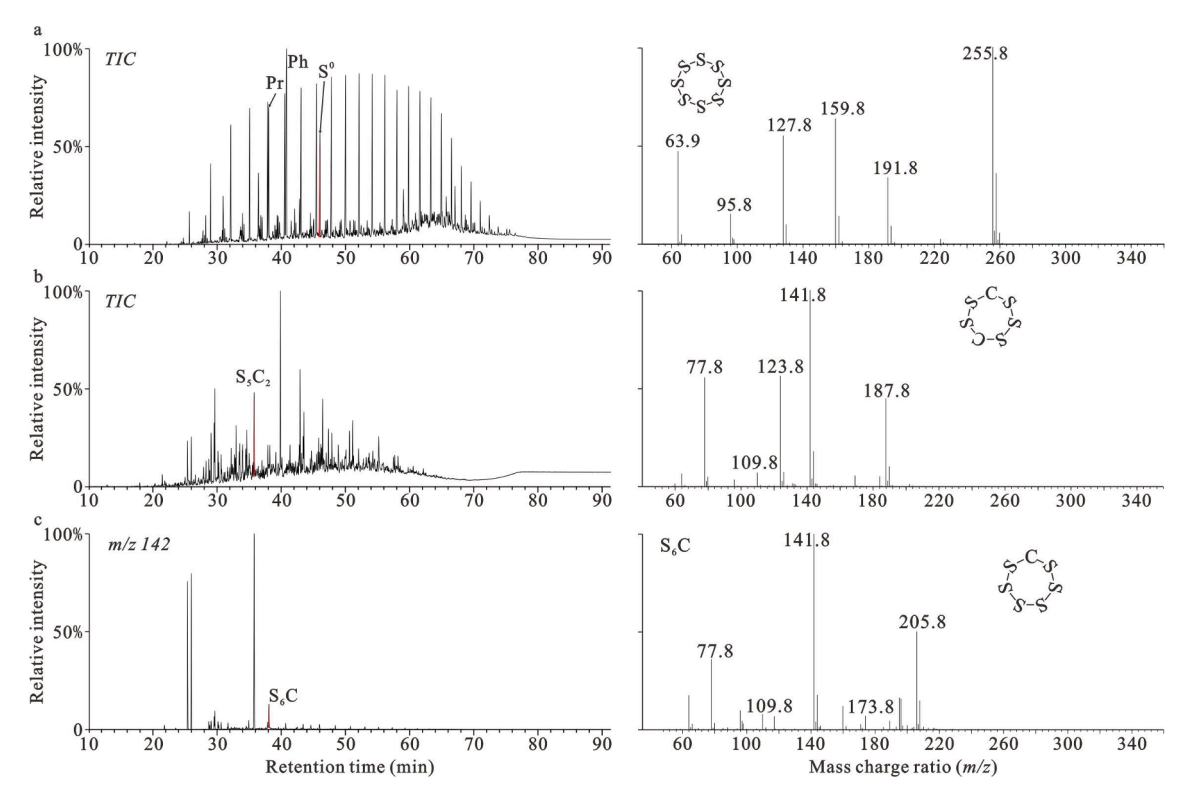


Fig. 4. Labile compounds detected by GC–MS. (a)  $S_8$  detected in the saturated hydrocarbons fraction, experiment Thio\_2; identification of (b) pentathiepane ( $S_5C_2H_4$ ) and (c) hexathiepane ( $S_6CH_2$ ) in aromatic hydrocarbon fraction, experiment Sulfite\_2. TIC = Total ion count.

levels of reactivity of the tested sulfur-containing species in these experiments follow the sequence:  $S^0 > S_2 O_3^{2-} \approx S_4 O_6^{2-} > SO_3^{2-} \approx SO_4^{2-}$ .

In the experimental conditions tested in this study, thermal degradation of hydrocarbons, ultimately generating methane and pyrobitumen, is expected to occur simultaneously with the targeted redox reactions. The relationship between CH<sub>4</sub> yield and the concentration of added sulfur (Fig. 1c) is not significant. However, Fig. 7b shows that within the compounds with the most experimental data (thiosulfate and tetrathionate experiments)  $\rm CO_2$  and  $\rm CH_4$  yields are indeed correlated.

#### 4.2. Labile sulfur species in altered crude oils

Significant amounts of elemental sulfur and unusual labile organo-sulfur compounds, tentatively identified from mass spectral data as pentathiepane ( $S_5C_2H_4$ ) and hexathiepane ( $S_6CH_2$ ), can be detected in the altered oils, but not in the original oil. These labile organosulfur compounds have been discovered in immature sediments [35,36] but their occurrence in crude oils has not been extensively reported. The occurrence of pentathiepane and hexathiepane in these altered oils suggests that these may be important intermediates in the process of crude oil oxidation with sulfur oxy anions. In particular, their occurrence in the oil altered by sulfite is remarkable in terms of their abundance, which may indicate the route of incorporation of sulfur into hydrocarbons and other species.

Polysulfide anions can in principle be formed during the oxidation of hydrocarbons by sulfate (GWB calculations:  $MgSO_4 \& 1-C_8H_{16}$ ; Table 5). In addition, large amounts of  $S_3^-$  ion have been reported during the process of TSR in geological fluids and in the laboratory by *in-situ* Raman spectroscopy [37,38]. Polysulfides have also been suggested as key intermediate-valence species involved in the TSR process, allowing for fast electron transfers [38]. The reaction with hydrocarbons to form polysulfide may be a major pathway for the incorporation of sulfur into organic matter. The formation of S-S bonds should be a necessary step followed by the generation of polysulfides. Thiosulfate and tetrathionate contain S—S bonds but given the lack of S-S bonds in sulfate and sulfite,

the discovery of organic polysulfides and elemental sulfur in altered oils requires the breaking of S—O bonds under high P-T. The high bond strength of S-O bond [125–132 kcal/mol; 39] makes the thermochemical sulfate reduction difficult to occur. For thiosulfate and tetrathionate, weaker S-S bonds may trigger the formation of polysulfide species more easily and then accelerate the whole reaction releasing much more  $H_2S$  [bond strength: 33–72 kcal/mol; 38,39].

#### 4.3. Compositional changes in altered oils

#### 4.3.1. Hydrocarbons

The hydrocarbon compound distribution in the altered oils differed from the original oil, but the real impact of the redox-promoted alterations is best assessed comparing altered oils to the pyrolyzed initial oil, reacted thermally without any added sulfur species (Oil 360 1). This comparison facilitates interpretations against a background of baseline thermal reactions occurring in the matrix. *n*-Alkane distributions are in general shifted towards lower molecular weight species, this being the most significant change seen for the experiment with S<sub>8</sub>. Also, in the oxidative conditions promoted by the added sulfur compounds, isoprenoid alkanes seem less stable than n-alkanes. Hydrocarbons, which account for > 50% of the total species intensity detected in (+) APPI FTICR-MS spectra, also change in distribution, shifting towards lower carbon numbers (e.g., peaks at  $C_{29} \rightarrow C_{19}$ ) in experiments with sulfur compounds, echoing the behavior of the n-alkanes seen in GC-MS analysis (Figs. 3 and 5d). On the other hand, the double bond equivalents (DBE) of detected hydrocarbon species in the altered oils increases with adding the sulfur compounds to the reaction chamber (Fig. 5e, peak at DBE 5  $\rightarrow$  13). Modified Kendrick plots shown in Fig. 8 highlight the general compositional trends of hydrocarbon compound alterations caused by addition of sulfur compounds. Experiments without added sulfur compounds show a wider range of carbon numbers for each DBE plot. For aromatic species, there should exist an upper aromaticity limit for each carbon number [40]. The polysulfide species may drive hydrocarbons undergoing accelerated dehydrogenation/aromatization to

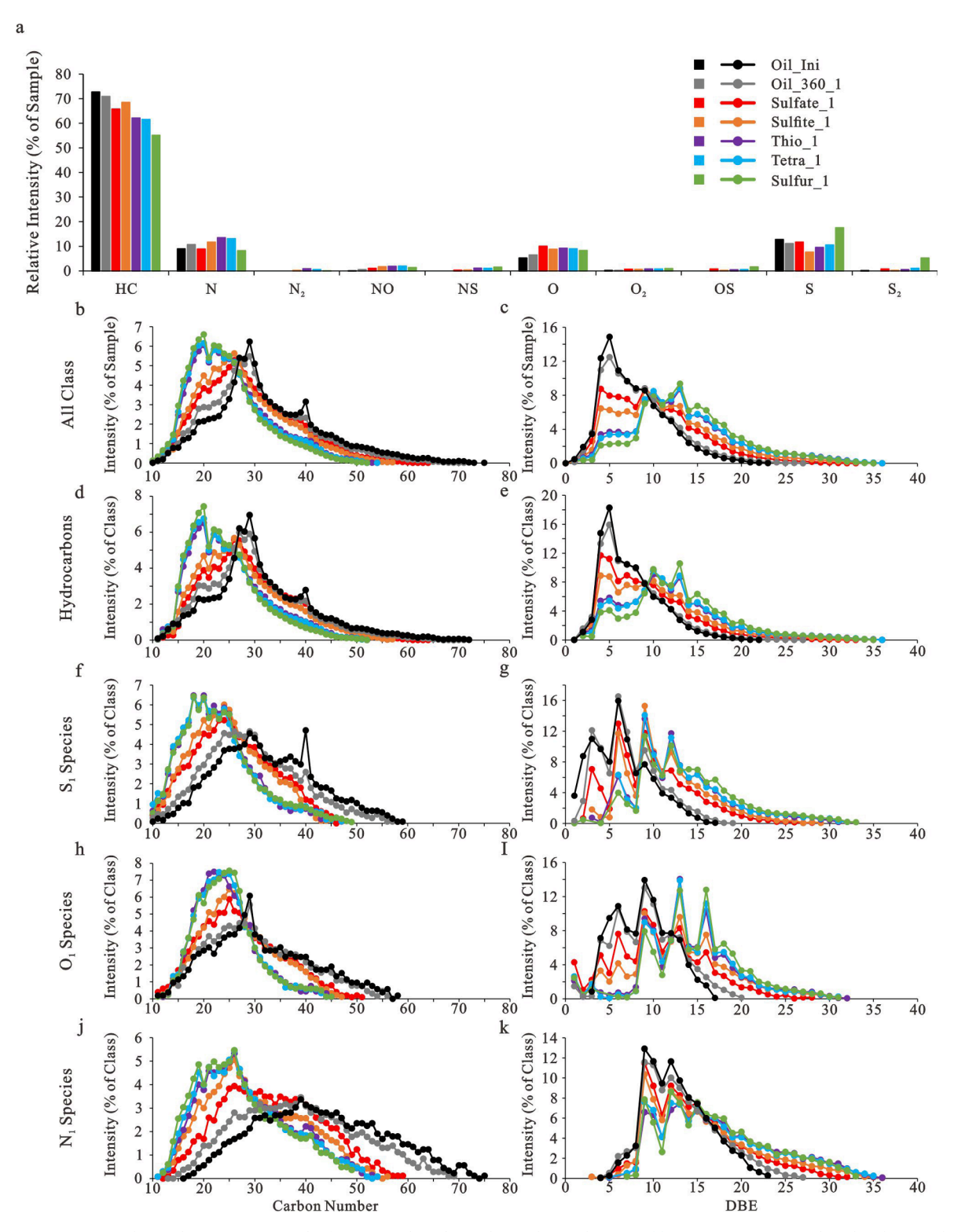


Fig. 5. (+) APPI FTICR-MS chemical composition results for seven selected samples in this study (see Table 2). (a) Heteroatom class distribution; (b-k) Carbon number and double bond equivalent (DBE) distribution of selected heteroatom classes. Y-axis represent the relative intensity of the species normalized either by sample or heteroatom class.

approach the limit of aromaticity, compared to the typical pyrolysis conditions without any sulfur species added. The cracking of C—C bonds occurred simultaneously yielding lower molecular weight species.

#### 4.3.2. S containing species in the modified crude oils

The (+) APPI FTICR-MS results presented herein (Fig. 5), include the detection of heteroatom classes  $S_1$  and  $S_2$  and enable a different

analytical perspective on studying sulfur incorporation into the organic matter during the sulfur species promoted redox reactions. The detection of S-bearing heteroatom species via (+) APPI FTICR-MS analysis of crude oils has been proposed to correlate with the sample total sulfur content [40,41]. It has long been known that TSR altered oils are enriched in organosulfur compounds [thiol, thiophene, dibenzothiophene; 8,9,21,42]. The formation of OSC is attributed to the back

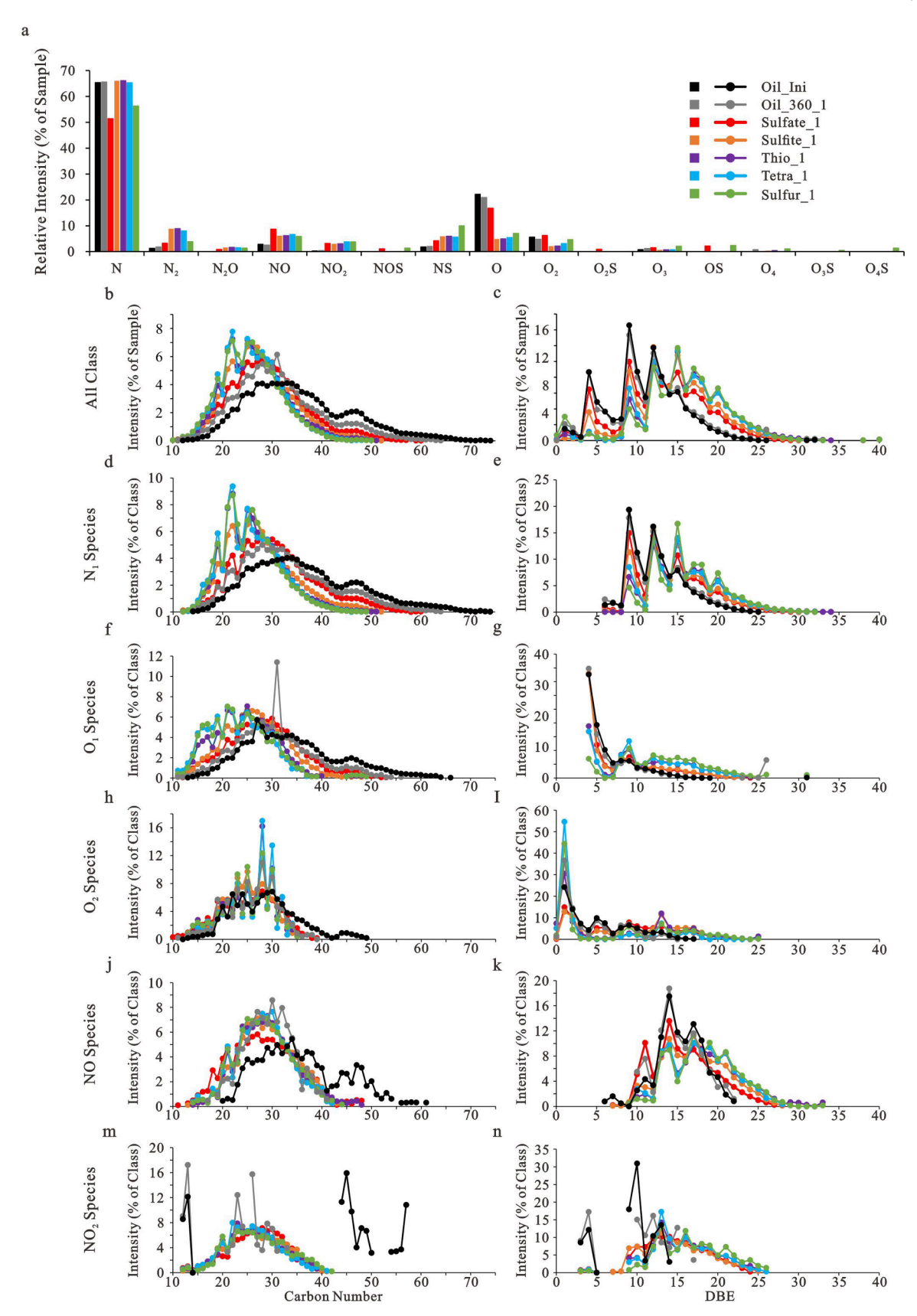


Fig. 6. (-) ESI FTICR-MS chemical composition results for seven selected samples in this study (see Table 2). (a) Heteroatom class distribution; (b-k) Carbon number and double bond equivalent (DBE) distribution of selected heteroatom classes. Y-axis represent the relative intensity of the species normalized either by sample or heteroatom class.

Table 5 Geochemist's Workbench calculations estimating the molality (the moles of solute in 1 kg of solvent; mol/kg) of sulfur oxy anion likely to exist in aqueous solutions at 360 °C, 450 bars after heating for 72 h. The initial molality of sulfur oxy anions  $(SO_4^2, SO_3^{2-}, S_2O_3^2, S_4O_6^2 \text{ and } S_8^0)$  and 1-Octene  $(C_8H_{16})$  in these model experiments were 1.47 mol/kg in water. Only species > 1E-08 molality listed. I.m. = Initial molality (mol/kg), I.s. = Initial solvent mass (g), S.m. = Solvent mass (g). \*Mass loss of  $Mg^{2+}$  due to the formation of  $Mg(CH_3COO)_2$ ,  $MgHCO_3^+$  and  $MgCH_3COO^+$ .

	MgSO <sub>4</sub>	MgSO <sub>4</sub> & 1-C <sub>8</sub> H <sub>16</sub>	$\mathrm{SO}_3^{2-}$	$S_2O_3^{2-}$	$S_4O_6^{2-}$	S <sup>0</sup>
I.m.	1.47	1.45	1.47	1.47	1.47	1.47
I.s.	1.00	1.00	1.00	1.00	1.00	1.00
S.m.	1.00	0.91	0.99	0.97	0.94	0.99
$MgSO_4$	1.43	5.12E-07				
$Mg^{2+}$	4.09E-02	7.87E-03*				
$SO_4^{2-}$	4.02E-02	2.13E-06	0.15	0.20	4.56E-02	6.74E - 07
HSO <sub>4</sub>	4.42E-04		2.61E-06	3.49E-02	2.09	1.78E-02
NaSO <sub>4</sub>			0.97	1.28	0.32	
SO <sub>2</sub> (aq)	9.00E-08			5.35E-04	0.96	0.42
$SO_3^{2-}$	1.32E-08		9.12E-07	6.42E-08		
$HSO_3^-$	2.41E-06		3.66E-07	2.55E-04	1.44E-03	1.19E-05
$S_2O_3^{2-}$	3.57E-08		1.92E-06	2.53E-03	8.71E-04	
$HS_2O_3^-$				1.37E-05	1.24E-03	4.26E-06
$S_4O_6^{2-}$				1.40E-06	0.15	1.63E-07
HS <sup>-</sup>	1.29E-04	1.16	0.37	3.60E-02	1.75E-04	1.14E-06
$H_2S(aq)$	1.04E-04	0.43	1.52E-03	1.47	2.23	0.90
$S_5^{2-}$				2.57E-04	3.07E-04	
S <sub>2</sub> <sup>2-</sup> S <sub>4</sub> <sup>2-</sup> S <sub>3</sub> <sup>2-</sup> S <sub>2</sub> <sup>2-</sup>				2.20E-04	1.64E-05	
$S_3^{2-}$		2.34E-06	4.33E-08	1.49E-04	6.92E - 07	
$S_2^{2-}$		5.67E-04	4.25E-04	7.81E-05	2.27E-08	

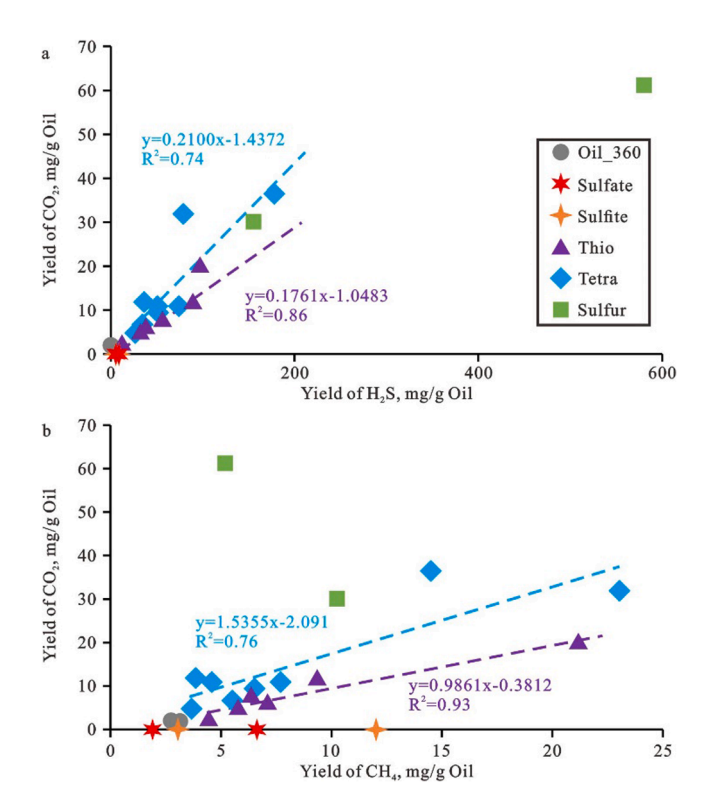


Fig. 7. Correlation between (a)  $CO_2$  and  $H_2S$ ; (b)  $CO_2$  and  $CH_4$  formation yields. Linear fit for the multiple tetrathionate and thiosulfate experiments are shown. Each experimental point represents one measurement.

reaction of  $H_2S$  with organic matter [8,17,43]. Interestingly, the relative intensity of  $S_1$  species in the altered-oils treated by sulfate, sulfite, thiosulfate and tetrathionate in our experiments are not significantly different [Fig. 5a; 20]. The sample treated with sulfite showed the lowest heteroatom class  $S_1$  relative ion intensity, whereas the oil altered by  $S_1$ 0 shows the highest relative intensity of sulfurized compounds (class  $S_1$ .2, Fig. 9). However, dibenzothiophene (DBT) and benzonaphthothiophene (BNT) are remarkably abundant in the oils altered by sulfur oxy anions (Table 4). We propose that the non-enrichment of the whole  $S_1$ 1 species in

oil treated by sulfate and sulfite (Table 4) may due to the lack of inorganic reduced sulfur incorporation (little  $\rm H_2S$  formed). Even though relatively large amounts of  $\rm H_2S$  were formed from experiments with thiosulfate and tetrathionate, (+) APPI data showed no evident large-scale sulfurization of the oil matrix (Fig. 5a). There may be a dynamic balance between sulfur incorporation and the decomposition of OSCs, since experiments have been done at high temperature conditions (compared to geological settings), where pyrolysis and net species decomposition is a dominant process. It is also unclear whether the final sulfurized species eventually generated under these conditions are dominantly within the analytical window of (+) APPI FTICR-MS, i.e. m/z > 150. The enrichment of  $\rm S_1$  species and  $\rm S_2$  species in oils altered with elemental sulfur is remarkable and those compounds also show the general trend of higher DBE and low carbon numbers for species in the altered oils (see Figs. 5 and 9).

The overall characteristics of the detected OSC in the altered oils are different based on the sulfur species present. In the samples pyrolyzed without sulfur oxy anions, elevated DBE 3 and 6 species relative intensities suggest that thiophene and benzothiophene homologs are likely the dominant compounds seen in heteroatom class S<sub>1</sub> (Fig. 5g). However, dibenzothiophene, benzonaphthothiophene and their homologs, with DBE of 9 and 12 are formed in oil altered by sulfur compounds, and fused ring aromatized OSC with higher DBE are also seen. Results shown in Fig. 9 further suggest that the altered oils tend to move to higher levels of net aromatization associated with shorter alkyl chain lengths. We proposed that the oxidation and thermochemical alteration may eliminate labile sulfur functional groups converting and preserving remnant sulfur species more as more stable aromatic structures such as DBT and BNT, leading to the accumulation of these more refractory OSCs. These highly aromatic species are mainly polycyclic thiophenes, likely formed by insertion of sulfur bridges into polycyclic aromatic hydrocarbons [44]. The GC-MS based proxy for sulfurization extent (DBT concentration) suggests the oil sulfurization ranking occurs in the order of decreasing sulfurization reactivity in the sequence  $S^0 > SO_3^{2-} > S_4O_6^{2-} \sim$  $S_2O_3^{2-} > SO_4^{2-}$ . As indicated before, sulfate, despite being the most abundant common sulfur oxy anion in subsurface waters, is the least reactive species with crude oil.

#### 4.3.3. O containing species in the altered crude oils

Modified Kendrick plots of class  $O_1$  species obtained with (+) APPI and (-) ESI ionization modes, shown in Fig. 10, suggest that the

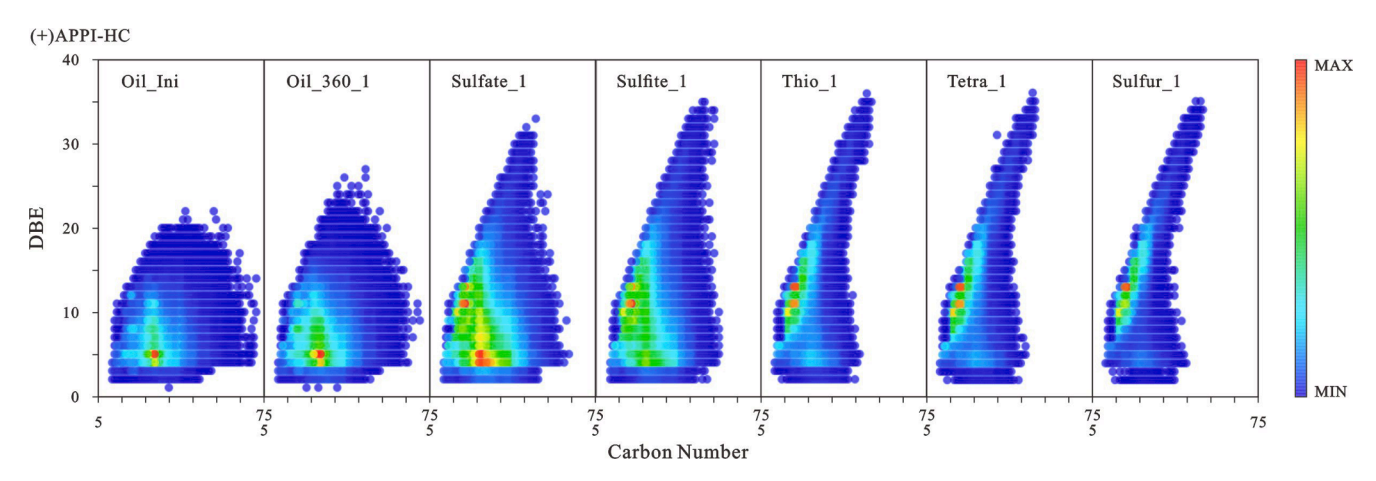


Fig. 8. Modified Kendrick plots for (+) APPI FTICR-MS class HC species. Data points are color-coded by their intensity relative to the maximum intensity in each sample.

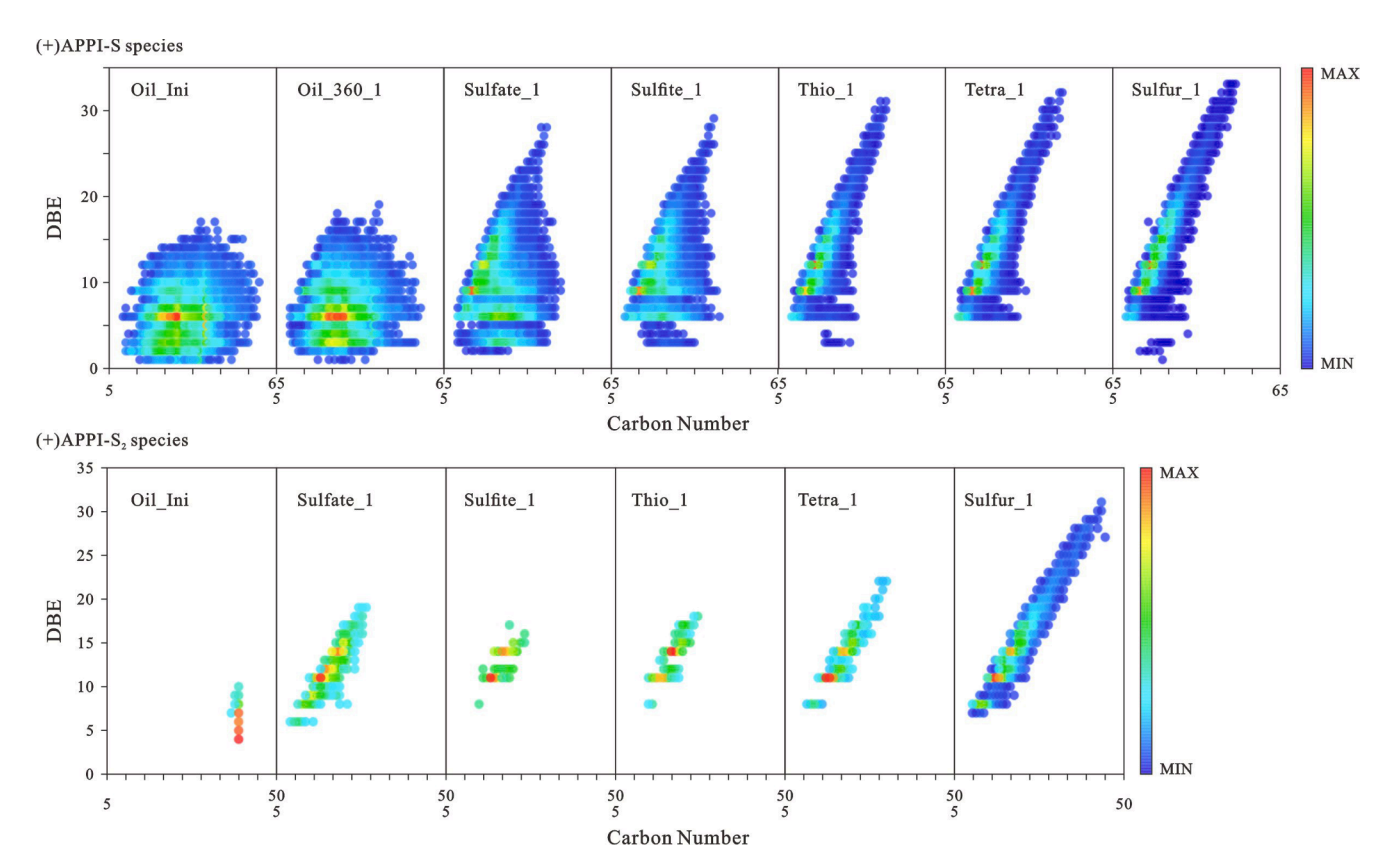


Fig. 9. Modified Kendrick plots for (+) APPI FTICR-MS class S and  $S_2$  species. Data points are color-coded by their intensity relative to the maximum intensity in each sample.

distribution of carbon numbers of  $O_1$  heteroatom class species in altered oils behaves in a similar manner to the  $S_1$  heteroatom class species previously discussed (Figs. 5 and 6f). In general terms, (+) APPI class  $O_1$  species shows a relative abundance increase in altered oils (Fig. 5a). The initial oil is rich in  $O_1$  species with DBE of 4–6 and 9, tentatively identified as phenols, benzofurans, dibenzofurans and their homologs. Whilst in oils altered with sulfur compounds, a predominance of  $O_1$  species with DBE of 9, 13 and 16 is observed, suggesting dibenzofuran, phenyl-dibenzofuran and phenyl-benzonaphthofuran species and their alkyl homologs (Fig. 5I) become more dominant. Even though the majority of species detected in the more altered matrix (oils treated with elemental sulfur, tetrathionate and thiosulfate) are DBE  $\geq 9$  (dibenzofurans), some species with DBE < 4 can still be detected in (+)

APPI mode (Fig. 10). Such DBE 1–3, labile oxygenated species, which can be inferred to likely represent aldehydes, alcohols, and/or ethers, are likely to be intermediates of the hydrocarbon oxidation processes promoted in these experiments. The relative enrichment of  $O_1$  species detected by (+) APPI (Fig. 5), seen in the experiments with added sulfur compounds, may be derived from the oxidation promoted by the oxy sulfur compounds.

The (-) ESI ionization mode is very efficient in detecting polar molecules able to deprotonate. Mainly,  $O_1$  species detected by (-) ESI spectra in crude oil samples are the more acidic phenols (DBE 4) and their homologs (see predominant DBE 4 signal in Fig. 6g). The (-) ESI class  $O_1$  species substantially decreased in relative intensity when oils are reacted with sulfur compounds. The detected species in highly

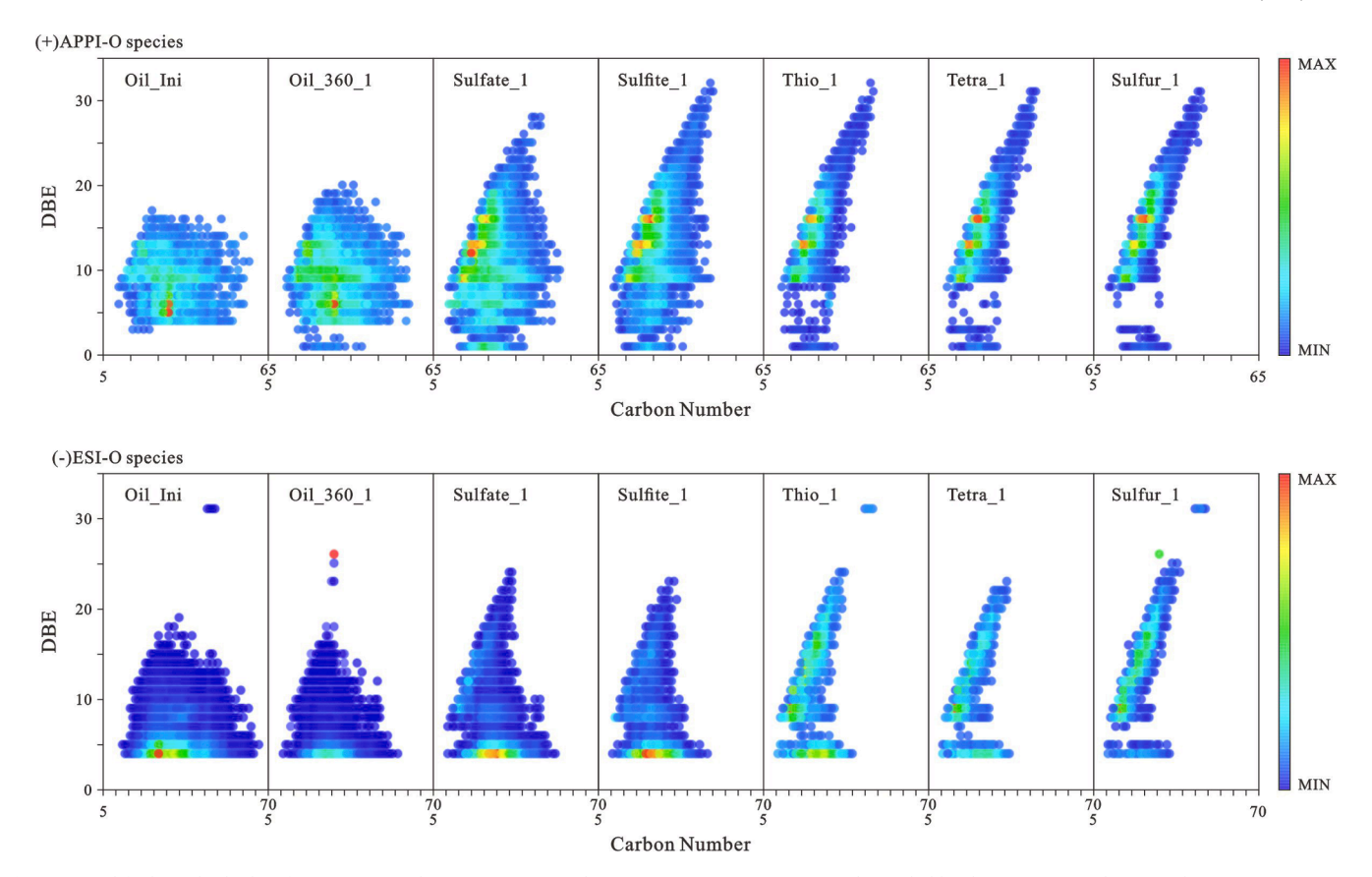


Fig. 10. Modified Kendrick plots for (+) APPI and (-) ESI FTICR-MS class O species. Data points are color-coded by their intensity relative to the maximum intensity in each sample.

altered oils (e.g. reacted with  $S^0$  in Fig. 10, ESI mode) are likely neoformed polycyclic aromatic compounds bearing a phenol group in one of the rings. Based on data from both modes, (+) APPI and (-) ESI, we observe that altered oils are leaner in phenol species and richer in oxygen-bearing higher DBE species, putatively furan-like, less labile molecules. This likely reflects relative stability of the different species during thermal alteration.

Although very low in relative intensity, results show that the (+) APPI Class O2 heteroatom class species are likely polycyclic furan-like aromatic compounds given their high DBE range (11-23). Regarding the (-) ESI O<sub>2</sub> heteroatom class data, observations similar to heteroatom class O<sub>1</sub> can be made (Fig. 11). In this case, however, molecule deprotonation (and thus enhanced detection), can also be driven by the presence of carboxyl groups. There is a ubiquitous detection of DBE 1-2 species in all the samples, likely carboxylic acids. The species close to the aromaticity limit may carry either a phenol or carboxyl group - experiments to determine this are beyond the scope of this first paper. We remind the reader that, common fatty acid contaminants detected in the solvent blank analysis have been removed from further processing – see Section 2.3, but contaminants from sample processing and handling have not been assessed. Based on Walters et al. findings [20], extensive oxygenation caused by the oxidation of aromatic rings would be expected in such sulfate mediated redox reactions. However, in this study, only heteroatoms of classes O<4 have been detected (Figs. 5, 6 and S4). The removal of labile oxygenated intermediates due to elevated thermal stress is the most likely explanation for such observations. In fact, considering the evidence that hydroxyl and carboxyl groups may decompose during the high P-T experiments, one would speculate that the highly oxygenated species generated during aromatic ring oxidation are intermediates and may ultimately contribute to CO2 formation.

#### 4.3.4. $N_1$ And $NO_{1-2}$ species

In crude oils, nitrogen-bearing functional groups are commonly either pyridinic or pyrrolic, both of which can be detected by (+) APPI. On the other hand, (-) ESI is more sensitive to the pyrrole/carbazolelike structures carrying an acidic hydrogen. Modified Kendrick plots of (+) APPI and (-) ESI class N<sub>1</sub> heteroatom species are shown in Fig. 12. Since there was no addition of nitrogen bearing reactants in our experiments, N-containing species are most likely native in the crude oil and the observed compositional changes seen are similar to those observed in the hydrocarbons, oxygen- and sulfur-bearing hetero-compounds. In (-) ESI, the elevated relative intensity of NO, NS, N<sub>2</sub> and NO<sub>2</sub> heteroatom species in altered-oils (except Oil\_360 where no sulfur species were added) is intriguing, although unassessed ionization response factors prevent us from pinpointing whether these species are indeed formed or simply had their detection enhanced after modifying the chemical matrix during the high P-T experiments. Still, we speculate that N-bearing species are being further oxidized and sulfurized in reactions with added sulfur bearing reactants, and the distribution of the NO and NO2 heteroatom species produced, could help us to understand the mechanisms of oxidation of organic matter in these environments. Fig. 13 indicates that NO and NO2 heteroatom species are likely alkylated polycyclic aromatic compounds and the oxygen-bearing functional groups are likely to be phenolic hydroxyl, aldehydes, furan-like species and carboxylic acids. The enrichment of these aromatic NO and NO2 heteroatom species may indicate the interaction of aromatic species and sulfur oxy anions under high P-T.

#### 4.4. Improved understanding of the TSR mechanism

The mechanism of thermochemical sulfate reduction has been extensively investigated [11,17,20,22]. Even though many studies had different approaches and results, the bond strength of S-O bonds in the

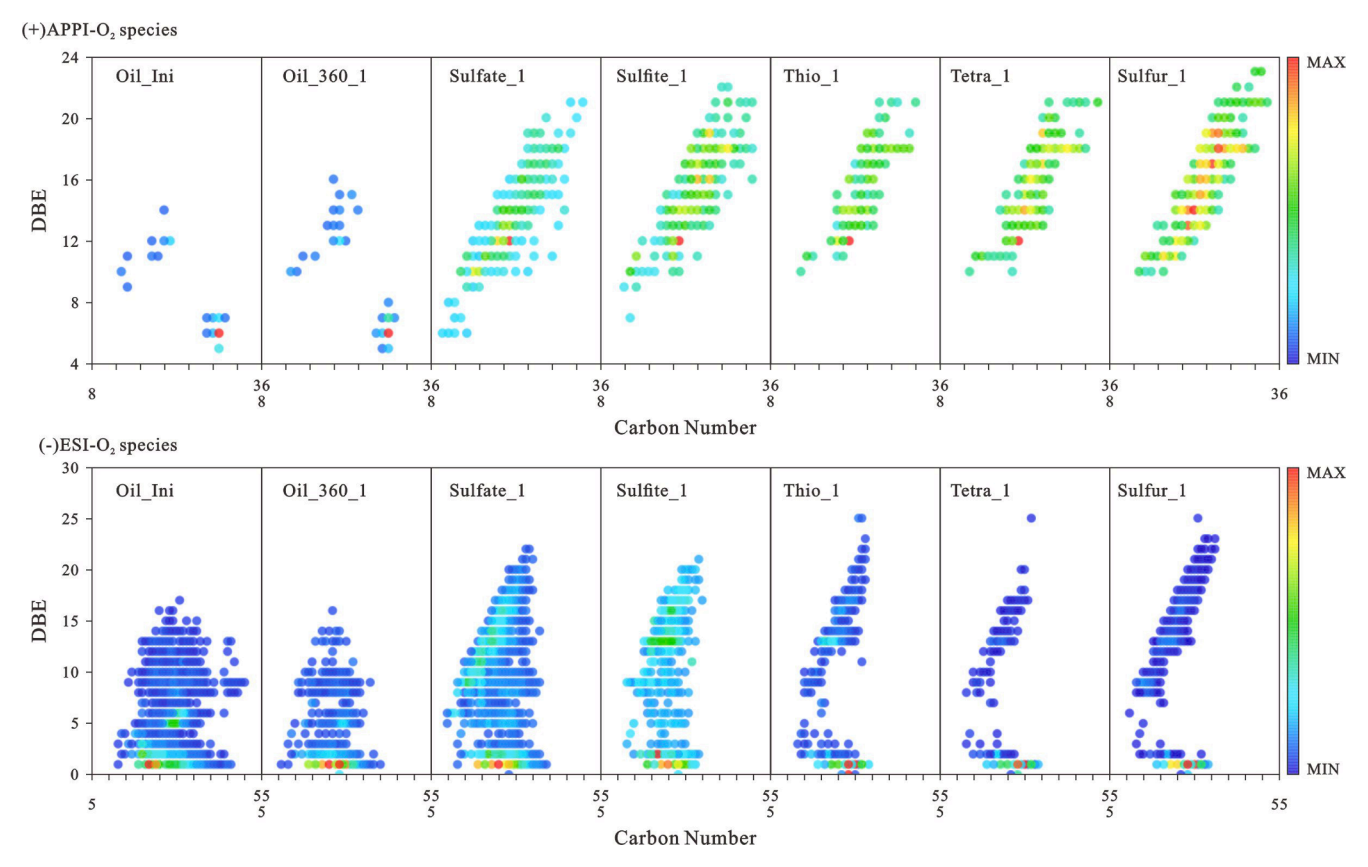


Fig. 11. Modified Kendrick plots for (+) APPI and (-) ESI FTICR-MS class O<sub>2</sub> species. Data points are color-coded by their intensity relative to the maximum intensity in each sample.

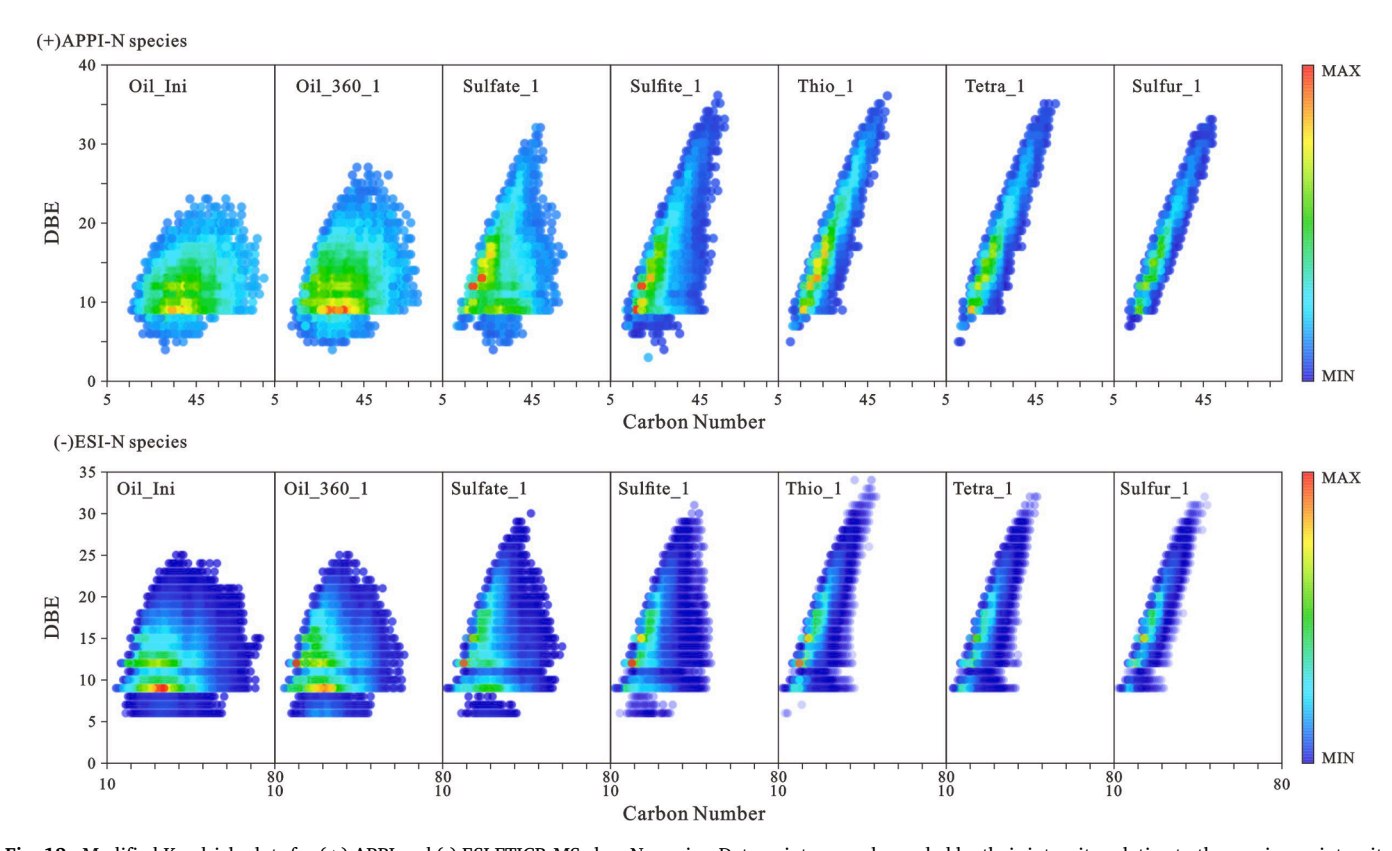


Fig. 12. Modified Kendrick plots for (+) APPI and (-) ESI FTICR-MS class N species. Data points are color-coded by their intensity relative to the maximum intensity in each sample.

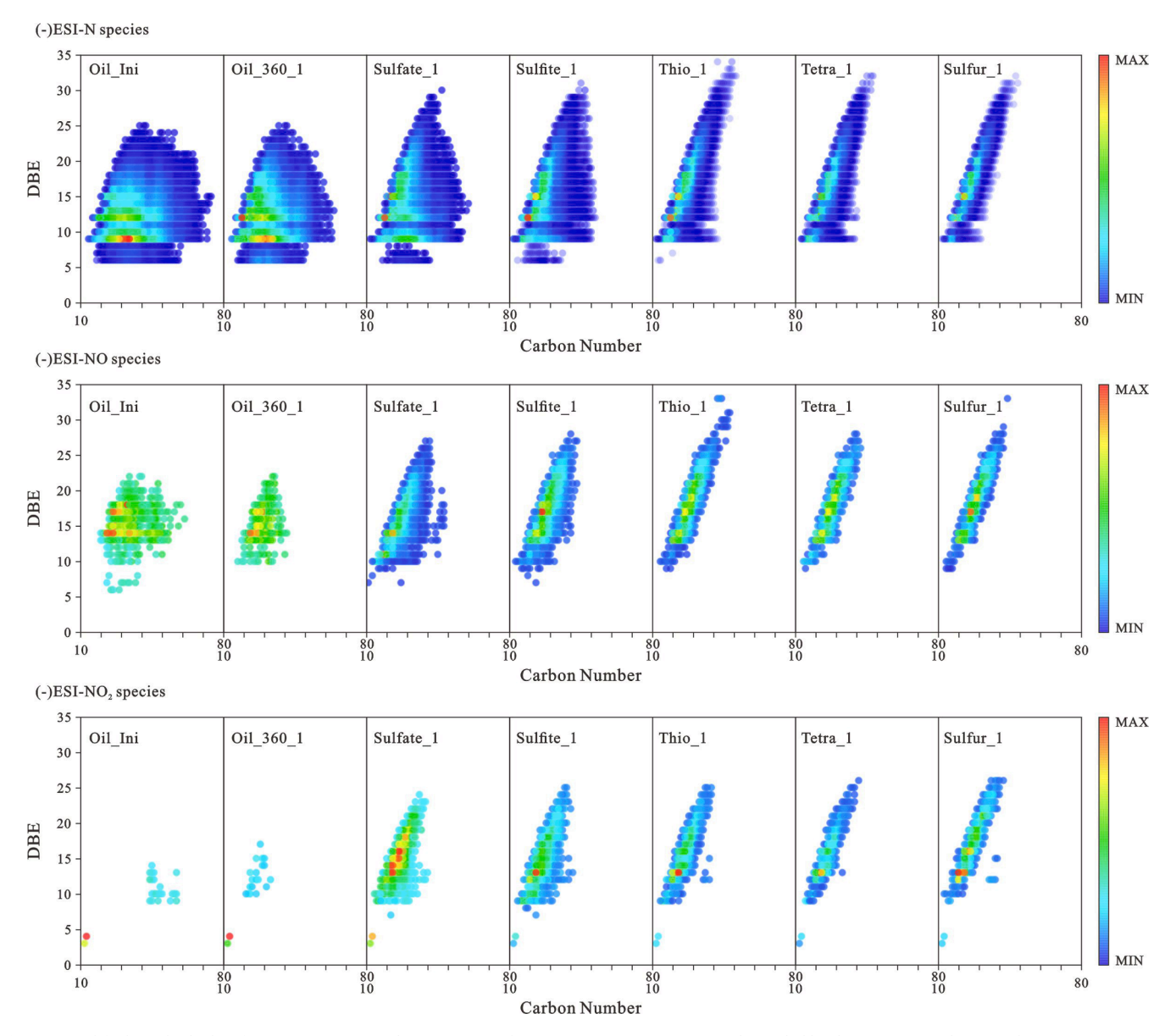


Fig. 13. Modified Kendrick plots for (-) ESI FTICR-MS classes N, NO and NO<sub>2</sub> species. Data points are color-coded by their intensity relative to the maximum intensity in each sample.

sulfate ion is suggested to be the main factor responsible for the relatively slow kinetics of TSR reactions [13,24,45,46]. The traditional view of TSR is that system pH and initial H<sub>2</sub>S concentrations greatly affect the rate of TSR and that the process is accelerated once sulfite is formed [13,17,37,38]. However, in the experimental conditions used in this study, added sulfite did not greatly promote the generation of H<sub>2</sub>S compared to other sulfur species, despite the notable occurrence of pentathiepane (S<sub>5</sub>C<sub>2</sub>H<sub>4</sub>) and hexathiepane (S<sub>6</sub>CH<sub>2</sub>) in the experiments. The efficiency of thiosulfate, tetrathionate and elemental sulfur in producing H<sub>2</sub>S may indicate that S-S bonds accelerate the whole redox reaction, which echoes the study from Truche et al. [38]. We propose that once polysulfide species accumulate, the net interaction between hydrocarbons and sulfur oxy anions would be fast. Whether radical mediated processes are important is uncertain.

Artificial maturation experiments in the laboratory surely differ from processes occurring in natural geological settings. Compared with our experiments, a wider carbon number distribution range and the occurrence of poly-oxygenated species has been reported in petroleum samples naturally altered by TSR [20]. In experiments reported herein, we propose the polyoxygenated species are short-lived intermediate species

that may undergo decarboxylation or other degradation process under the high P-T conditions of our experiments. The apparent formation of saturated fatty acids and  $O_2$ , NO and  $NO_2$  aromatic heteroatom species may indicate the direct oxidation of saturated and aromatic hydrocarbons or heteroatom compounds. The oxidation of aromatic species may lead to aromatic ring-opening (as proposed in [20]), followed by decarboxylation forming  $CO_2$  as a final product.

### 4.5. Assessment of possible routes to in situ fossil fuel energy recovery approaches using reactive sulfur electron shuttles

Thermochemical sulfate reduction is detrimental to petroleum reservoirs, forming  $H_2S$  which is toxic and corrosive and a threat to human health and the environment. However, the interaction between reactive sulfur species in petroleum in reservoirs is a potential technological route to energy recovery at the surface, from petroleum reservoirs with zero  $CO_2$  emission, via the energy vector hydrogen sulfide [1,3]. Biological routes to sulfate reduction by hydrocarbons at large scale are limited by the toxicity of sulfide ion to biological systems. In contrast, abiotic chemical routes such as TSR like processes will not have such

limits, though other substantial practical issues remain. In this study, we artificially altered the crude oil at high temperature using five different oxidation states of S species. Elemental sulfur, thiosulfate, and tetrathionate are the most reactive species and efficiently extract hydrogen from hydrocarbons and water to form H2S. Obviously, the reactions in our experiments are taking place at high temperatures for any plausible subsurface engineered processes, so there would be substantial engineering challenges or the need for development of very effective catalysts before anything approaching a realistic technology might even be considered. However, such proposed approaches might be capable of generating hydrogen sulfide at scale, the H2S being transported to the surface and oxidized with atmospheric oxygen, either in a furnace for process heat or for generating power in a fuel cell or even providing fuel hydrogen by decomposition of the H<sub>2</sub>S [47]. The re-oxidized shuttle (for example, thiosulfate or tetrathionate) might be recirculated back to the reservoir via water floods (Fig. 14). In such schemes, the energy in the oil reservoir is harvested for electricity, heat or hydrogen via the H2S acting as a shuttle, while the CO2 produced during hydrocarbon oxidation, is trapped in the reservoir formation either as a gas phase or via carbonate precipitate depending on reservoir geochemical conditions. Table 6 shows the enthalpy changes for the oxidation of C<sub>4</sub>H<sub>8</sub> and H<sub>2</sub>S which were performed using SUPCRT92 and Gaussian 09 [30,48]. Oxidation of hydrocarbons with sulfur species is exothermic and thus might support a high-temperature in situ reaction based process. As expected, oxidation of hydrocarbons or hydrogen sulfide, with oxygen is also exothermic. H<sub>2</sub>S could be an energy vector instead of hydrocarbons for the recovery of fossil fuel energy. In terms of petroleum substrates, there are a few advantages of considering such a system: (a) reservoirs with low oil saturation can be utilized; (b) virtually any form of hydrocarbon can be used as substrate; (c) the petroleum industry has great expertise in dealing with H2S. Further, some H2S using fuel cells have been investigated [49,50]. There is clearly much uncertainty regarding the plausibility, feasibility or even desirability of the system, in terms of kinetics, thermodynamics and engineering realities and the reactions here were carried out at very high temperatures. There are existing processes for high-temperature recovery of crude oil from reservoirs that operate at temperatures as high as this, but without some means to accelerate the process at lower temperatures the practicality of the approach seems limited. We have not investigated the efficiency or energy balance of the approach and this study has shown that not all sulfur

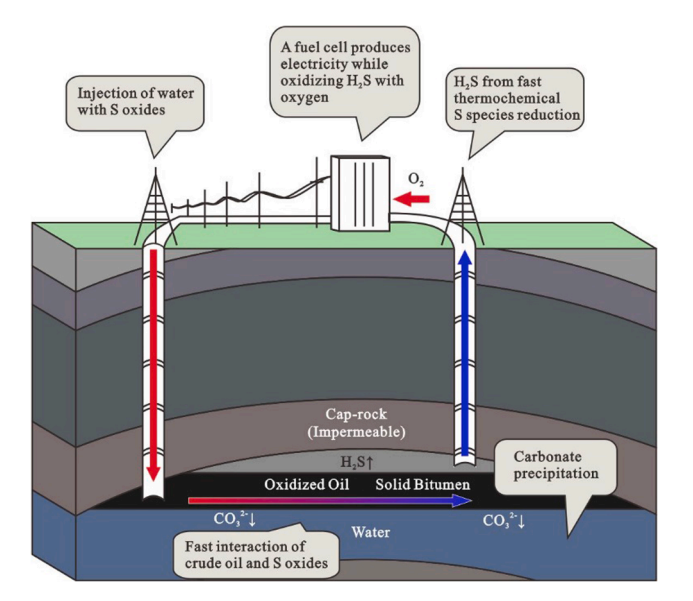


Fig. 14. A potential scheme of energy harvesting using fast thermochemical S species reduction.  $CO_2$  produced in the reservoir remains trapped in situ. (after Novotnik et al, 2020). It is not clear if such processes would be feasible at reasonable insitu temperatures.

**Table 6**Enthalpy and Gibbs free energy change in these three redox reactions. The pressure is 450 bars. Calculations were performed using SUPCRT92 and Gaussian 09.

Reaction	T °C	ΔH kcal/ mol	ΔG kcal/ mol
$C_4H_8 + 6O_2 = 4CO_2 + 4H_2O$	150 350	-659.03 $-722.85$	-635.50 -616.03
$\begin{array}{l} C_4 H_8 + 3 S_2 O_3^{2-} {+} 3 H_2 O = 4 C O_3^{2-} + 2 H^+ + \\ 6 H_2 S \end{array}$	150 350	-23.90 $-63.75$	-19.72 $-14.74$
$2H_2S + 3O_2 = 2SO_2 + 2H_2O$	150 350	-330.82 $-327.38$	-322.55 $-318.83$

species are equal in terms of reactivity. Clearly any practical or plausible technology is a long way from reality, and the social and political desirability of such a technology also needs to be considered, but further examination of kinetics, thermochemistry, catalysis systematics and engineering practicalities of such approaches may be worthy of some thought as the world urgently seeks to decarbonize in the next few decades.

#### 5. Conclusion

As part of a program examining the development of alternative energy vectors to recover fossil fuel energy without atmospheric composition impacts, in this study we investigated the high P-T chemical oxidation of crude oil with a suite of inorganic sulfur compounds to draw insights on plausibility of using  $H_2S$  as an energy vector or hydrogen scavenger to recover energy from petroleum reservoirs without any associated carbon. Based on the experimental results, the following conclusions can be drawn:

The sulfur compounds we tested, can be ordered by the ability to promote chemical changes to the oil matrix, in a sequence of decreasing reactivity, S  $^0$  > S2O3 $^2$  ~ S4O6 $^2$  > SO3 $^2$  > SO4 $^2$  . We propose that the  $S^0$ ,  $S_2O_3^{2-}$  and  $S_4O_6^{2-}$  species are much more reactive due to the labile S-S bonds present in these compounds, which can easily form polysulfides, promoting the alteration of hydrocarbons. In high *P-T* conditions, hydrogen could be extracted efficiently from both hydrocarbons and water by the added sulfur species to form H<sub>2</sub>S at a higher yield than CO<sub>2</sub>. Dehydrogenation occurred in altered oils by reactive sulfur oxy anions. Questions can be raised as to whether further focus on new ways of using petroleum resources distracts from more rapid moves to renewable energy resources, but we felt small scoping studies were needed at this time. Although toxic and generally undesirable, H<sub>2</sub>S is a potential energy vector if the general research and development mindset shifts from avoiding it to using its chemical versatility in a safe manner. It is also not clear whether such an approach would be socially acceptable even if engineered in a safe manner.

Organic and inorganic polysulfide species are likely key intermediates in the process of crude oil oxidation by sulfur oxy anions. Although the altered oils are rich in DBT, BNT and their homologs, the relative intensity of heteroatom classes  $S_1$  and  $S_2$  do not increase significantly, as detected by (+) APPI FTICR-MS. The incorporation of sulfur into organic matter driven by the reduction of sulfur oxy anions is limited. The accumulation of aromatic organosulfur compounds, such as DBTs and BNTs, may derive from the conversion and concentration of more labile organic sulfur species, rather than predominantly from the incorporation of new inorganic sulfur.

The apparent formation of saturated fatty acids and  $O_2$ , NO and  $NO_2$  aromatic heteroatom species indicates that sulfur oxy anion oxidized hydrocarbons could act on both saturated and aromatic species. The oxidation of aromatic species may lead to aromatic ring-opening, followed by decarboxylation forming  $CO_2$  as final products. The

removal of labile poly-oxygenated intermediates in artificial maturation experiments may be due to elevated thermal stress.

#### **Declaration of Competing Interest**

The authors declare that they have no known competing financial interests or personal relationships that could have appeared to influence the work reported in this paper.

#### Acknowledgements

Shengbao Shi, Lei Zhu and Shuo Gao are thanked for their help with the experimental program in CUP-Beijing. Priyanthi Weerawardhena and Melisa Brown are thanked for their contribution to sample analyses in Calgary. We thank Bruker for support of the Calgary FTMS facility. Thomas Oldenburg and Aphorist Inc. are thanked for the FTICR-MS analytical and software support. This research was made possible in part by research support from National Natural Science Foundation of 41403049), the China Scholarship (No.201906440182), Canada First Research Excellence Fund (CFREF), UCalgary Global Research Initiative in Low Carbon Unconventional Resources, Canada Foundation for Innovation (CFI), the joint China University of Petroleum and University of Calgary Shengli oilfield project, PRG and the University of Calgary. At last, the first author Xiao Jin would like to thank the patience, care and support from Yinan He as a companion all the way and would you please marry him?

#### Contribution statement

This study was conceived and designed by XJ, JW, NZ, RCS and SRL with supporting discussions and key inputs from HH and ZZ. XJ and ZZ carried out the laboratory experiments, analysis and data interpretation. FTICR-MS data processing was carried out by RCS, and data interpretation was carried out by both XJ and RCS. XJ and RCS drafted the manuscript. BMT and XJ contributed with GWB simulations. JW, SRL and HH assisted with sample collection and geochemical discussions. All authors revised the manuscript.

#### Appendix A. Supplementary data

Supplementary data to this article can be found online at https://doi.org/10.1016/j.fuel.2021.121050.

#### References

- [1] Novotnik B, Nandy A, Venkatesan SV, Radović JR, Fuente JDl, Nejadi S, et al. Can fossil fuel energy be recovered and used without any CO2 emissions to the atmosphere? Rev Environ Sci Bio/Technol 2020;19(1):217–40. https://doi.org/10.1007/s11157-020-09527-z.
- [2] Head IM, Jones DM, Larter SR. Biological activity in the deep subsurface and the origin of heavy oil. Nature 2003;426(6964):344–52. https://doi.org/10.1038/ nature02134.
- [3] Park M, Ryu J, Wang W, Cho J. Material design and engineering of next-generation flow-battery technologies. Nat Rev Mater 2017;2(1). https://doi.org/10.1038/ natrevmats.2016.80.
- [4] Novotnik B, Zorz J, Bryant S, Strous M. The effect of dissimilatory manganese reduction on lactate fermentation and microbial community assembly. Front Microbiol 2019;10. https://doi.org/10.3389/fmicb.2019.01007.
- [5] Borowski WS, Rodriguez NM, Paull CK, Ussler W. Are 34S-enriched authigenic sulfide minerals a proxy for elevated methane flux and gas hydrates in the geologic record? Mar Pet Geol 2013;43:381–95. https://doi.org/10.1016/j. marnetyeo.2012.12.009.
- [6] Fernandes NA, Gleeson SA, Magnall JM, Creaser RA, Martel E, Fischer BJ, et al. The origin of Late Devonian (Frasnian) stratiform and stratabound mudstone-hosted barite in the Selwyn Basin, Northwest Territories, Canada. Mar Petrol Geol 2017; 85:1–15. https://doi.org/10.1016/j.marpetgeo.2017.04.006.
- [7] Inagaki, F., et al. Exploring deep microbial life in coal-bearing sediment down to ~2.5 km below the ocean floor. Science. 2015;349(6246):420. doi:10.1126/ science.aaa6882.
- [8] Amrani A. Organosulfur compounds: molecular and isotopic evolution from biota to oil and gas. Annu Rev Earth Planet Sci 2014;42(1):733–68.

- [9] Cai C, Worden RH, Bottrell SH, Wang L, Yang C. Thermochemical sulphate reduction and the generation of hydrogen sulphide and thiols (mercaptans) in Triassic carbonate reservoirs from the Sichuan Basin, China. Chem Geol 2003;202 (1-2):39–57.
- [10] Hu W-X, Kang X, Cao J, Wang X-L, Fu B, Wu H-G. Thermochemical oxidation of methane induced by high-valence metal oxides in a sedimentary basin. Nat Commun 2018;9(1). https://doi.org/10.1038/s41467-018-07267-x.
- [11] Meshoulam A, Ellis GS, Said Ahmad W, Deev A, Sessions AL, Tang Y, et al. Study of thermochemical sulfate reduction mechanism using compound specific sulfur isotope analysis. Geochim Cosmochim Acta 2016;188:73–92. https://doi.org/ 10.1016/j.gca.2016.05.026
- [12] Zhang S, Huang H, Su J, Liu M, Wang X, Hu J. Geochemistry of Paleozoic marine petroleum from the Tarim Basin, NW China: Part 5. Effect of maturation, TSR and mixing on the occurrence and distribution of alkyldibenzothiophenes. Org Geochem 2015;86:5–18. https://doi.org/10.1016/j.orggeochem.2015.05.008.
- [13] Zhang T, Ellis GS, Ma Q, Amrani A, Tang Y. Kinetics of uncatalyzed thermochemical sulfate reduction by sulfur-free paraffin. Geochim Cosmochim Acta 2012;96:1–17. https://doi.org/10.1016/j.gca.2012.08.010.
- [14] Zhu G, Huang H, Wang H. Geochemical significance of discovery in cambrian reservoirs at well ZS1 of the Tarim Basin, Northwest China. Energy Fuels 2015;29 (3):1332–44. https://doi.org/10.1021/ef502345n.
- [15] Amrani A, Deev A, Sessions AL, Tang Y, Adkins JF, Hill RJ, et al. The sulfur-isotopic compositions of benzothiophenes and dibenzothiophenes as a proxy for thermochemical sulfate reduction. Geochim Cosmochim Acta 2012;84:152–64. https://doi.org/10.1016/j.gca.2012.01.023.
- [16] Krouse HR, Viau CA, Eliuk LS, Ueda A, Halas S. Chemical and isotopic evidence of thermochemical sulphate reduction by light hydrocarbon gases in deep carbonate reservoirs. Nature 1988;333(6172):415–9. https://doi.org/10.1038/333415a0.
- [17] Zhang T, Amrani A, Ellis GS, Ma Q, Tang Y. Experimental investigation on thermochemical sulfate reduction by H 2S initiation. Geochim Cosmochim Acta 2008;72(14):3518–30.
- [18] Ellis GS, Said-Ahmad W, Lillis PG, Shawar L, Amrani A. Effects of thermal maturation and thermochemical sulfate reduction on compound-specific sulfur isotopic compositions of organosulfur compounds in Phosphoria oils from the Bighorn Basin, USA. Org Geochem 2017;103:63–78. https://doi.org/10.1016/j. orggeochem.2016.10.004.
- [19] Zhu G, Wang M, Zhang T. Identification of polycyclic sulfides hexahydrodibenzothiophenes and their implications for heavy oil accumulation in ultra-deep strata in Tarim Basin. Mar Pet Geol 2016;78:439–47. https://doi.org/ 10.1016/j.marpetgeo.2016.09.027.
- [20] Walters CC, Wang FC, Qian K, Wu C, Mennito AS, Wei Z. Petroleum alteration by thermochemical sulfate reduction – A comprehensive molecular study of aromatic hydrocarbons and polar compounds. Geochim Cosmochim Acta 2015;153:37–71. https://doi.org/10.1016/j.gca.2014.11.021.
- [21] Li S, Shi Q, Pang X, Zhang B, Zhang H. Origin of the unusually high dibenzothiophene oils in Tazhong-4 Oilfield of Tarim Basin and its implication in deep petroleum exploration. Org Geochem 2012;48:56–80. https://doi.org/ 10.1016/j.orgeochem.2012.04.008
- [22] Xia X, Ellis GS, Ma Q, Tang Y. Compositional and stable carbon isotopic fractionation during non-autocatalytic thermochemical sulfate reduction by gaseous hydrocarbons. Geochim Cosmochim Acta 2014;139:472–86. https://doi. org/10.1016/j.gca.2014.05.004.
- [23] Goldstein TP, Aizenshtat Z. Thermochemical sulfate reduction a review. J Therm Anal 1994;42(1):241–90.
- [24] Ma Q, Ellis GS, Amrani A, Zhang T, Tang Y. Theoretical study on the reactivity of sulfate species with hydrocarbons. Geochim Cosmochim Acta 2008;72(18): 4565–76. https://doi.org/10.1016/j.gca.2008.05.061.
- [25] Lewan MD, Kotarba MJ, Curtis JB, Wiecław D, Kosakowski P. Oil-generation kinetics for organic facies with Type-II and -IIS kerogen in the Menilite Shales of the Polish Carpathians. Geochim Cosmochim Acta 2006;70(13):3351–68. https://doi.org/10.1016/j.gca.2006.04.024.
- [26] Zhang T, Ellis GS, Wang K-S, Walters CC, Kelemen SR, Gillaizeau B, et al. Effect of hydrocarbon type on thermochemical sulfate reduction. Org Geochem 2007;38(6): 897–910.
- [27] He K, Zhang S, Mi J, Zhang W. The evolution of chemical groups and isotopic fractionation at different maturation stages during lignite pyrolysis. Fuel 2018;211: 492–506. https://doi.org/10.1016/j.fuel.2017.09.085.
- [28] Huang H, Zhang S, Su J. Pyrolytically derived polycyclic aromatic hydrocarbons in marine oils from the tarim basin, NW China. Energy & Fuels 2015;29(9):5578–86. https://doi.org/10.1021/acs.energyfuels.5b01007.
- [29] Bethke CM, editor. Geochemical and Biogeochemical Reaction Modeling. Cambridge: Cambridge University Press; 2007.
- [30] Kong X-Z, Tutolo BM, Saar MO. DBCreate: a SUPCRT92-based program for producing EQ3/6, TOUGHREACT, and GWB thermodynamic databases at userdefined T and P. Comput Geosci 2013;51:415–7. https://doi.org/10.1016/j. cageo.2012.08.004.
- [31] Shock EL, Sassani DC, Willis M, Sverjensky DA. Inorganic species in geologic fluids: correlations among standard molal thermodynamic properties of aqueous ions and hydroxide complexes. Geochim Cosmochim Acta 1997;61(5):907–50. https://doi. org/10.1016/S0016-7037(96)00339-0.
- [32] Shock EL, Helgeson HC. Calculation of the thermodynamic and transport properties of aqueous species at high pressures and temperatures: standard partial molal properties of organic species. Geochim Cosmochim Acta 1990;54(4):915–45. https://doi.org/10.1016/0016-7037(90)90429-O.

- [33] Robinson BW. Sulphur isotope equilibrium during sulphur hydrolysis at high temperatures. Earth Planet Sci Lett 1973;18(3):443–50. https://doi.org/10.1016/ 0012-821X(73)90101-5.
- [34] Webster JG. Thiosulphate in surficial geothermal waters, North Island, New Zealand. Appl Geochem 1987;2(5):579–84. https://doi.org/10.1016/0883-2927 (87)90010-2
- [35] Kawka OE, Simoneit BRT. Survey of hydrothermally-generated petroleums from the Guaymas Basin spreading center. Org Geochem 1987;11(4):311–28. https://doi.org/10.1016/0146-6380(87)90042-8.
- [36] Kohnen MEL, Sinninghe Damsté JS, Ten Haven HL, kock.-Van Dalen AC, Schouten S, De Leeuw JW. Identification and geochemical significance of cyclic diand trisulphides with linear and acyclic isoprenoid carbon skeletons in immature sediments. Geochim Cosmochim Acta 1991;55(12):3685–95. https://doi.org/ 10.1016/0016-7037(91)90067-F.
- [37] Pokrovski GS, Dubrovinsky LS. The S<sub>3</sub><sup>—</sup> Ion is stable in geological fluids at elevated temperatures and pressures. Science 2011;331 (6020):1052–4. https://doi.org/10.1126/science.1199911.
- [38] Truche L, Bazarkina EF, Barré G, Thomassot E, Berger G, Dubessy J, et al. The role of S-3 ion in thermochemical sulphate reduction: geological and geochemical implications. Earth Planet Sci Lett 2014;396:190-200. https://doi.org/10.1016/j.com/2014.04.018
- [39] Ohmoto H, Lasaga AC. Kinetics of reactions between aqueous sulfates and sulfides in hydrothermal systems. Geochim Cosmochim Acta 1982;46(10):1727–45. https://doi.org/10.1016/0016-7037(82)90113-2.
- [40] Marshall AG, Rodgers RP. Petroleomics: chemistry of the underworld. PNAS 2008; 105(47):18090-5.
- [41] Corilo YE, Rowland SM, Rodgers RP. Calculation of the total sulfur content in crude oils by positive-ion atmospheric pressure photoionization fourier transform ion cyclotron resonance mass spectrometry. Energy Fuels 2016;30(5):3962–6. https:// doi.org/10.1021/acs.energyfuels.6b00497.

- [42] Orr WL. Changes in sulfur content and isotopic ratios of sulfur during petroleum maturation—Study of big horn basin paleozoic oils1. AAPG Bull 1974;58(11): 2295–318. https://doi.org/10.1306/83d91b9b-16c7-11d7-8645000102c1865d.
- [43] Wei Z, Mankiewicz P, Walters C, Qian K, Phan NT, Madincea ME, et al. Natural occurrence of higher thiadiamondoids and diamondoidthiols in a deep petroleum reservoir in the Mobile Bay gas field. Organic Geochem ORG GEOCHEM 2011;42 (2):121–33. https://doi.org/10.1016/j.orggeochem.2010.12.002.
- [44] White CM, Douglas LJ, Schmidt CE, Hackett M. Formation of polycyclic thiophenes from reaction of selected polycyclic aromatic hydrocarbons with elemental sulfur and/or pyrite under mild conditions. Energy Fuels 1988;2(2):220–3.
- [45] He K, Zhang S, Mi J, Ma Q, Tang Y, Fang Yu. Experimental and theoretical studies on kinetics for thermochemical sulfate reduction of oil, C2–5 and methane. J Anal Appl Pyrol 2019;139:59–72. https://doi.org/10.1016/j.jaap.2019.01.011.
- [46] Kiyosu Y, Krouse HR. The role of organic acid in the abiogenic reduction of sulfate and the sulfur isotope effect. Geochem J 1990;24(1):21–7. https://doi.org/ 10.2343/geochemj.24.21.
- [47] Cox BG, Clarke PF, Pruden BB. Economics of thermal dissociation of H2S to produce hydrogen. Int J Hydrogen Energy 1998;23(7):531–44. https://doi.org/ 10.1016/S0360-3199(97)00111-0.
- [48] Zhao Y, Truhlar DG. The M06 suite of density functionals for main group thermochemistry, thermochemical kinetics, noncovalent interactions, excited states, and transition elements: two new functionals and systematic testing of four M06-class functionals and 12 other functionals. Theor Chem Acc 2008;120(1): 215–41. https://doi.org/10.1007/s00214-007-0310-x.
- [49] Kakati BK, Kucernak ARJ. Gas phase recovery of hydrogen sulfide contaminated polymer electrolyte membrane fuel cells. J Power Sour 2014;252:317–26. https://doi.org/10.1016/j.jpowsour.2013.11.077.
- [50] Cavalli A, Bernardini R, Del Carlo T, Aravind PV. Effect of H2S and HCl on solid oxide fuel cells fed with simulated biosyngas containing primary tar. Energy Sci Eng 2019;7(6):2456–68. https://doi.org/10.1002/ese3.v7.610.1002/ese3.434.